Modelling and Analysis of Leaching of Copper from Volcanic Ash Soil

A thesis presented in partial fulfilment of the

requirments for the degree of **Master of Technology**

in **Environmental Engineering**

by **Dali He**

Institute of Technology and Engineering

Massey University

Palmerston North, New Zealand

1999

ABSTRACT

Soil contaminated by heavy metal ions has become a global problem. Besides legislation to restrict the input of heavy metals, remediation of contaminated soil is also essential. The most common means of remediation is leaching. There have been many studies published in this field, some of which relate to development of mathematical models. Volcanic ash soil is common in New Zealand. Developing a model to predict the process of leaching heavy metal from volcanic ash soil is important for New Zealand. No model was found for predicting the process of leaching heavy metal from volcanic ash soil.

Heavy metal soil contamination can not be remedied by microorganisms, so the heavy metals will inevitably accumulate in soils over time. Once heavy metals have accumulated in soil to exceed a threshold, they will be released and then be taken up by plants, entering the food chain or moving into the groundwater system. Therefore, it is necessary to leach the heavy metals from the contaminated soil. The batch stirred process is a fast and convenient method, and it is easily used in the field. The main purpose of this study is to develop a model that can predict the bulk liquid concentration of heavy metal in the stirred vessel.

In the present study, the internal model is pore diffusion model. The explicit method is used to translate a partial differential equation to a finite difference equation. The results from thermodynamic and kinetic experiments agree with the model. With the exception of the equilibrium parameters for Freundlich isotherm derived by experiment, all other parameters were obtained from literature on volcanic ash soil. Therefore, the model can be used for leaching of other heavy metals from volcanic soil under similar conditions.

The leaching of heavy metals from volcanic soil is shown to be an internal diffusion controlled process, so increasing the agitating speed in a stirred reactor is of no use for improving the mass transfer. Decreasing the size of volcanic soil

aggregates by breaking them clearly increases the rate of the leaching process. The equilibrium relationships of the adsorption process and the desorption process are different for the system, and there is a hysteresis.

ACKNOWLEDGEMENTS

I wish to express my sincere gratitude to my chief supervisor Prof. S. M. Rao Bhamidimarri for his assistance, valuable advice and guidance during this study, and writing of this thesis.

I am very grateful also to my co-operative supervisor Ken Butler for valuable assistance in experiments, literature review and writing of this thesis.

Thanks to John Sykes for valuable help on using Atomic Absorption Spectrophotometer.

Finally, I would like to thank all of those people who have helped with this project.

CONTENTS

LIST OF FIGURES

LIST OF TABLES

CHAPTER 1

INTRODUCTION

1.1 Background

The distribution of soils derived from volcanic materials closely parallels the global distribution of active and recently active volcanoes. It is estimated that soils derived from volcanic ejecta are distributed over approximately 124 million hectares or 0.84% of the earth's surface (Leamy, 1984). Approximately 60% of volcanic ash soils occur in tropical countries. In some countries with high volcanic activity, there may be a higher distribution of volcanic ash soils such as Japan, Melanesia, and Philippines.

Volcanic ash soil is also common in New Zealand. Most of the region south from Auckland to Wanganui on the west coast, and to Napier on the east coast, has a mantle of volcanic ash deposits more than 18 inches thick (Gibbs, 1968). The occurrence of volcanic soil is shown by the numerous particles of volcanic glass found in most soils of the North Island. The presence of volcanic ash soil has made New Zealand a favourable country for the production of food, timber, and water.

With wide application of sewage sludge and some chemical products including pesticides and herbicides to agricultural land, the risk and extent of soil contamination has increased. The pollutants in contaminated soils can be divided into two groups, organic matter and heavy metals. Organic pollutants include pesticides and herbicides. They can be degraded or decomposed by microorganisms in soil. However, microorganisms can not decompose heavy metals. Therefore, heavy metals will inevitably accumulate in soils over time. Once heavy metals have accumulated to exceed a threshold, they will be released and then be taken up by plants, entering the food chain

or moving into the groundwater system. Consequently, human health and the environment in which human lives may be seriously imperiled. It may be necessary to leach heavy metals from contaminated soil.

1.2 Remediation technologies

There are many technologies to remedy contaminated soil. Koustas and Fischer (1998) indicated that the various available treatment options for remediation fall into three broad categories: containment-immobilization, separation-concentration, and destruction. Each category can be classified by different ways in which technique can be used as in situ, a prepared bed, and in tank (Boulding, 1995).

- In situ treatment consists of treating contaminated soil in place, i.e., the contaminated soil is not moved from the ground. Although the treatment method is the best way in economic terms, there are some restricting conditions and potential new damage to soil for this method.

- In a prepared bed system, the contaminated soil may be either (1) physically moved from its original site to a newly prepared area, which has been designed to enhance treatment and/or to prevent transport of contaminants from the site; or (2) removed from the site to a storage area while the original location is prepared for use, then returned to the bed, where treatment is accomplished. The advantages and disadvantages of the method are not conspicuous.

- In tank treatment involves removing the contaminated soil and treating it in a vessel or other system designed to optimize treatment efficiency. The method needs more operation cost, but there is no potential of new pollution to soil and fewer restricting requirements.

The heavy metals in contaminated soil cannot be destroyed by thermal treatment and microorganism because their ions can not be degraded. Therefore, just containment-

immobilization and separation-concentration can be considered. However, soil immobilization may result in the significant change on physical and chemical properties of soil. The result is that soil loses its agricultural function. Because soil is a limited resources on earth, the economical factor of soil remediation may be no longer a restrictive aspect for mankind in the near future. Thus, the method of separation-concentration in tank may become a principal aspect in soil remediation.

The main principle of remedying soil contaminated by heavy metal is leaching using a solvent. The solvent may be water, organic or inorganic reagent. There are many processes, which can be used to leach heavy metals from contaminated soil. For example, there are fixed bed or fluidized bed systems, continuous or batch processes. This work uses a batch stirred process.

1.3 Objectives of the project

The main purpose of this study is to develop a model that can predict the bulk liquid concentration of heavy metal in the stirred tank reactor. During the operation of leaching heavy metals from contaminated soil, monitoring heavy metal concentration in the bulk liquid is a regular practice in order to determine whether the bulk liquid concentration of heavy metal has achieved the required value. However, a large amount of monitoring work in the field is neither economical nor convenient. On the contrary, using a model to predict the concentration can be very easy, and only the initial concentrations of heavy metal in the bulk liquid need to be determined during the experiment.

A mathematical model has been developed. Experimental work on adsorption and desorption parameter determination and leaching in a stirred tank reactor is presented. The reliability of the models is discussed.

CHAPTER 2

LITERATURE REVIEW

2.1 Introduction

Soils formed from volcanic ash are known to be different from other mineral soils under similar climate conditions in morphological, mineralogical, chemical and physical properties (Wada, 1985). During the last forty years, volcanic ash soils have been studied by many researchers, both in New Zealand and overseas, using a wide range of techniques, and some general features of volcanic ash soils have been formulated. However, some important properties of volcanic ash soils such as tortuosity have not been studied because of difficult measurement.

Volcanic ash soils display a wide range of chemical and physical properties. Of these chemical properties, soil organic matter, active aluminum and iron, and variable charge are the most prominent attributes regulating chemical reactions in volcanic soils. Some physical characteristics of volcanic ash soils are obviously different from those of other soils, such as lower bulk density.

Because volcanic ash is a porous medium and has a large specific surface area, it can be used as an adsorbent for organic matter and heavy metals. Therefore, adsorption equilibria and process kinetics will also be reviewed in this chapter.

2.2 Volcanic ash soil

The term, volcanic ash soils, is commonly used to designate soils formed from tephras or pyroclastic materials (Shoji et al., 1993). Since most of these soils have unique

properties inherited from or associated with the properties of tephra, the general term, volcanic ash soils, is often used to denote andosols (FAO/Unesco, 1974) and andisols (Soil Survey Staff, 1990 and 1992). However, not all volcanic ash soils are andosols or andisols and vice versa. Shoji et al. (1993) summarized the central concept for volcanic ash soil as follows:

(1). The parent material is mostly pyroclastic material.

(2). The soil material contains an appreciable amount of allophane which is a series of naturally occurring noncrystalline and hydrous aluminosilicates, and shows low bulk density, and

(3). The soil material is mostly vitric.

2.2.1 Volcanic soil genesis

The effects of volcanic ash on soil formation depend primarily on the thickness and frequency of the ash showers. On those sites where the ash deposit is deep, or it accumulates rapidly so as to smother the vegetation and bury the previous soil to a depth of 2 ft or more, soil formation has to begin again. Where volcanic ash deposits are only shallow, or accumulate slowly by thin increments to a considerable depth, any disturbance of the vegetation is slight and interruption to the organic cycle is temporary (Gibbs, 1968).

Volcanic ash or tephra is commonly unconsolidated, comminuted material containing a large quantity of volcanic glass that shows little resistance to chemical weathering. Therefore, tephras weather rapidly resulting in formation of large amounts of noncrystalline materials. This process occurring preferentially in tephras was first called andosolization by Duchaufour (1984).

Andisols can be formed in tephras by andosolization in a relatively short time under most climates throughout the world. However, not all andisols are derived from tephra and not all tephra-derived soils are andisols. There are some nontephra-derived andisols

(Garcia-Rodeja et al., 1987; Hunter et al., 1987) and transition of andisols to most soil orders can occur, over time due to climatic factors affecting soil formation.

Such formation of noncrystalline materials is not specific to andisols. It is also widely observed for tephra-derived spodosols making it difficult to separate andisols and tephra-derived spodosols on the basis of solid-phase chemical criteria (Shoji and Ito, 1990).

2.2.2 Volcanic soils classification

New Zealand has developed its own national classification system for volcanic ash soils. Volcanic ash soils in New Zealand differ mainly in properties that are related either to the period of soil formation or to the composition of the parent ashes. Hence they are classed either as azonal or intrazonal soils associated with either central or northern yellow-brown earths (Gibbs, 1968).

Five groups are recognized and their interrelationships are seen by considering them in two sequences. The first sequence consists of groups 1 (in part), 2, 3, and 4, derived from rhyolitic and andesitic ashes; the other sequence consists of group 1 (remaining part) and subdivisions of group 5, derived from basaltic ashes (Gibbs, 1968). The five groups are:

(1) Recent Soils from Volcanic Ash

These are soils that have accumulated within historic times and have only two soil horizons. Their properties are considered to be determined principally by time (maximum age 500-700 years). Overseas they would be included in Regosols and Vitrandepts.

(2) Yellow-Brown Pumice Soils

These are soils formed from rhyolitic ash showers erupted during the last 3,000-5,000 years. These soils have either two or three soil horizons, and have pieces of pumice in the upper soil. Their properties are considered to be determined

principally by the parent materials. Overseas they would be included in Latosolic Brown Forest Soil and Normandepts.

(3) Yellow-Brown Loams

These are soils formed from either rhyolitic or andesitic ashes erupted between approximately 5,000 and 20,000 years ago. They have three horizons with high proportions of amorphous clays. In overseas classifications these soils are included in Andosols, Humic Allophane Soils, and Normandepts.

(4) Brown Granular Loams

These are soils formed from either rhyolitic or andesitic ashes erupted between approximately 20,000 and 100,000 years ago. They have three horizons, which contain more crystalline clays than amorphous clays. In overseas classifications these soils are included in Andosols, Reddish Brown Lateritic Soils, and Ultisols.

(5) Red Loams and Brown Loams

These are soils formed from basaltic ashes erupted before historic times. Their profiles have three horizons, containing amorphous clays and free oxides of iron and aluminum. Age sequences, in which there are decreases in the amounts of amorphous clays and increased segregation of oxides in forms such as gibbsite, have been identified in the field. Intermediate stages are difficult to map out owing to rapid soil development in finely divided materials, which have a high proportion of easily weathered minerals. In overseas classifications the red loams would be classed as Kraznosems and the brown loams as Latosolic Soils, Reddish Brown Lateritic Soils, and Hydrandepts.

2.2.3 Volcanic soil structure

Most soils are heterogeneous porous media that consist of aggregates and macropores between the aggregates. Soil structure is the arrangement of primary soil particles into secondary particles, units, or peds (Shoji et al., 1993). Structure changes with horizon,

organic matter content, soil texture, soil moisture content, etc. Andisols have various types of soil structure such as granular, angular blocky, subangular blocky, platy, or prismatic.

Noncrystalling materials and soil organic matter greatly contribute to the formation and stabilization of the soil structure. For example, Egashira et al. (1983) showed that water-stable aggregates greater than 53 μm in Japanese Andisols contain organic matter concentrations of 2.8 – 35.3 percent and clay contents of 11.9 – 71.1 percent. It is well known that soil moisture or alternate wetting and drying has a strong effect on aggregate formation (Shoji et al., 1993). The size distribution of soil aggregates is more closely related to pore size distribution and water retention than to particle-size distribution (Wu et al., 1990).

2.2.4 Volcanic soil constituents

Volcanic ash soils display a wide range of chemical and physical characteristics that strongly reflect the influence of the constituents of volcanic ash soils. Therefore, the constituents of volcanic ash soils are the basis that determines their chemical and physical characteristics. Volcanic ash soils consist of inorganic and organic matter. Organic matter influences many soil chemical and physical properties and enhances soil biological activity and productivity. Inorganic constituents affect the variable charge characteristics and adsorption-desorption behavior of volcanic ash soils.

2.2.4.1 Inorganic constituents

Inorganic constituents of volcanic ash soils affect its variable charge characteristics. Therefore, the cation exchange capacity of volcanic ash soils will be affected by their inorganic constituents.

All the volcanic ashes are lower in Boron than the average value for the lithosphere in New Zealand; mainly because the average value is dominated by the values for

sedimentary rocks, particularly greywacke (Gibbs, 1968). Differences in element content between topsoil and subsoil are very slight in the pumice soils (rhyolitic ash), primarily because the materials are only weakly weathered (Gibbs, 1968). Table 2-1 shows the micro-elements (Gibbs, 1968).

Table 2-1 Spectrographic analyses of volcanic soils

Depth	Horizon	Fe	Mn	Ba	Sr	Ga	V	Cr	Co	Ni	Cu	Zn	Mo	Ti
(in.)		(%)	ppm											
Ngauruhoe sand from Ngauruhoe ashes														
1-5	AC	5	1500	850	1000	14	200	150	20	10	60	150	2	3000
7-12	C	5	1500	900	1000	12	200	150	20	10	60	150	2	3000
Rotomahana sandy loam from Rotomahana mud														
0-1	A	3	1300	2100	860	9	70	2.5	5	1	13	260	1.5	1500
12-24	C	3	1000	2500	860	10	80	2	5	1	15	250	2	2000
Rangitoto sandy loam from Rangitoto ash														
0-5	A	8	400	500	1000	25	200	250	100	120	80	500	1	1000
Tarawera gravelly sand from Tarawera gravelly ash														
0-6	AC	8	4000	400	2000	30	400	50	100	3	30	200	3	10000
Burrell gravelly sand from Burrell gravelly ash														
0-6	AC	5	1000	2000	1500	30	300	30	25	10	100	300	2	5000

From Gibbs (1968).

Tephra, as a parent material, controls soil formation more than any other parent material and the major soil forming process taking place in tephra has been termed andosolization. Shoji et al. (1993) summarized the inorganic constituents of tephras from Japan and listed in Table 2-2.

Table 2-2 Content of major elements in fresh tephras from Japan

Element	Range (%)
SiO_2	48-73
Al_2O_3	12-20
Fe_2O_3 + FeO	2-12
TiO_2	0.4-1.2
CaO	2-11
MgO	0.5-8
K_2O	0.1-4
Na_2O	1.5-5

From Shoji et al. (1993).

2.2.4.2 Organic constituents

Soil organic matter plays an anti-allophanic role by forming aluminum-humus complexes under udic soil moisture regimes, strongly suggesting that nonallophanic andisols can accumulate more organic carbon than allophanic andisols (Shoji et al., 1993). Humus, as well as noncrystalline clay materials, contributes to the unique chemical and physical properties of Andisols such as variable charge (increases the negative charge and decreases the positive charge), high phosphate retention (reaction with the complex of aluminum-humus), low bulk density, notable friability, weak stickiness, formation of stable soil aggregates, etc. Humus also greatly influences the productivity of Andisols through its role in supplying nutrient elements, retaining available water for plants, and development of a favorable rooting environment (Shoji et al., 1993).

Accumulation of humus constituents is one of the features of Andisols. Suryaningtyas (1998) indicated that the interactions of allophane with organic matter in Andisols might be classified into four groups, *i.e.* (1) possible effects of allophane on the action of enzymes, (2) a catalytic effect of allophane in an oxidative polycondensation of phenolic units, which results in formation of stable skeletons in soil humic materials, (3) as a source of aluminum and/or iron which form insoluble humates, (4) the adsorption of humic materials. Organic matter is probably adsorbed onto allophane surfaces by ligand exchange.

2.2.5 Mineralogical characteristics of volcanic soil

A distinctive feature of soils derived from volcanic materials is the occurrence of a unique clay-size mineral assemblage dominated by noncrystalline components. Noncrystalline materials common in volcanic ash soils include: allophane, imogolite, opaline silica, and ferrihydrite. These materials can not be defined as "crystalline minerals" because they do not have a fixed chemical composition or a regular three-dimensional structural framework (Shoji et al., 1993).

Shoji et al. (1993) reported that the mineralogical composition of the colloidal fraction of soils derived from volcanic materials varies widely depending on (1) chemical, mineralogical, and physical properties of the parent material, (2) post-depositional weathering environment, and (3) the stage of soil formation. The mineralogy, chemical composition, and texture of the parent material largely determine the rate of chemical weathering, the amount and distribution of reactants for synthesis of secondary materials, and the pH is important through its influence on the base status of the soil.

2.2.5.1 Primary minerals

The primary mineral composition of volcanic ash is typically characterized by first dividing minerals into light (specific gravity [SG] < 2.8-3.0) and heavy (SG > 2.8-3.0) mineral categories (Shoji et al., 1993). Light minerals dominate in volcanic ash with an abundance mostly ranging between 70 and 95% (Shoji, 1986). Within the light mineral category, the relative abundance generally follows:

Noncolored volcanic glass >> **plagioclase feldspars** >> **silica minerals (quartz, cristobalite tridmite)** ≈ **mica**

The distribution of plagioclase and alkali feldspars is dependent on the chemical composition of the magma and is therefore quite variable. Heavy minerals comprise only a small fraction of volcanic ash having a felsic or intermediate chemical composition. The relative abundance of minerals within the heavy mineral category follows:

Hypersthene ≈ **opaque minerals** > **augite** ≈ **hornblende**

Shoji et al. (1993) indicated that the mineralogical composition of volcanic ash varies widely as a function of particle-size. Crystalline minerals are most common in the size range 100-500 μm. Plagioclase shows a relative uniform distribution throughout the silt and sand size fractions. In contrast, the heavy mineral content shows a pronounced decrease with decreasing particle size, until heavy minerals are virtually absent in the size

fractions less than 50 μm. Volcanic glass increases in relative proportion to plagioclase and heavy minerals as the particle size decreases.

Volcanic ash may also contain appreciable quantities of minerals that originate from previously altered minerals associated with the volcano (Shoji et al., 1993). These minerals, often called accessory, accidental or exotic minerals, are formed by weathering and/or hydrothermal alteration of minerals comprising the cone of the volcano. The accessory minerals along with the minerals formed from solidification of the magma are mixed and deposited together during a volcanic eruption. Accessory minerals attributed to previously altered minerals often include: opal, cristobalite, kaolinite, allophane, halloysite, smectite and interstratified layer silicates (Ossaka, 1982).

2.2.5.2 Secondary minerals

The secondary minerals of volcanic ash include allophane, imogolite, opaline silica, halloysite and non-crystalline iron oxide.

Allophane is a group name given to a series of naturally occurring, noncrystalline, hydrous aluminosilicates with a widely varying chemical composition (Van Olphen, 1971) and is also characterized by short range order (Parfitt, 1990). Order is the highest unit in the classification system of soil, so short range order indicates a group having the same original materials and chemical components. Based on the varying ratio of aluminum to silicon, allophanes found in New Zealand can be operationally divided into three main types (Parfitt, 1990). They are:

① Al-rich allophane (Al:Si molar ratio ≈ 2.0 or more);

② Si-rich allophane (Al:Si molar ratio ≈ 1.0);

③ Stream deposit allophane (Al:Si molar ratio ≈ 0.9-1.8).

The first two are predominant in soils. Allophane consists of hollow, irregularly spherical particles with outside diameters of 3.5 to 5 nm and a wall thickness of 0.7-1 nm (Shoji et al., 1993).

Imogolite was first described by Yoshinaga and Aomine (1962) in a soil derived from the glassy volcanic ash, known as "imogo". Imogolite commonly has been found in association with allophane and is similar to allophane in many of its chemical properties (Shoji et al., 1993). Imogolite is a short range order, hydrous aluminosilicate mineral with a distinct tubular morphology that may extend several microns in length from 100-300 Å. Imogolite consists of bundles of well-defined fine tubes with inner and outer diameters of about 7-10 Å and 17-21 Å, respectively (Suryaningtyas, 1998).

Two types of opaline silica are common in young volcanic ash soils: pedogenic opaline silica (commonly called laminar opaline silica) and biogenic opaline silica (plant opal and diatoms) (Shoji et al., 1993). Laminar opaline silica appears as a common constituent of the clay-size fraction in surface horizons of young volcanic ash soils (Shoji and Masui, 1971). Opaline silicas occur only in the 0.2-5 μm size fraction and are most abundant in the 0.4-2 μm range. Opaline silica is found more abundantly in younger soils (< 4000 years) than in older soils and in humus-rich A horizons rather than underlying B and C horizons.

Halloysite is common constituent in volcanic ash derived soils and occurs as the dominant clay mineral in many silicon-rich environments (Parfitt and Wilson, 1985). Halloysite is a 1:1 aluminosilicate mineral that is characterized by a diversity of morphology (Shoji et al., 1993). Generally it occurs with a tubular and spheroidal morphology in Andisols, but lath-shaped, platy, and crumpled shapes have also been reported (Nagasawa, 1978; Saigusa, 1978; Wada and Mizota, 1982; Nagasawa and Noro, 1987). Halloysite usually appears as unique spherules with diameters of 0.1-0.5 μm (Parfitt and Webb, 1984). Halloysite often occurs in older tephras, therefore it has been suggested that allophane weathers to halloysite with time. The apparent transformation of allophane into halloysite cannot be expressed as a simple function of time (Nagasawa, 1978). Halloysite can also form directly from volcanic glass where silica activity in soil solution is high (Parfitt and Webb, 1984).

Iron in soils derived from volcanic materials is present mostly in the form of

noncrystalline oxyhydroxides and partly as Fe-humus complexes (Parfitt and Childs, 1983; Parfitt et al., 1988; Childs et al., 1991). The dominant noncrystalline oxyhydroxide is believed to be ferrihydrite, a short-range-order iron hydoxide mineral with a bulk composition of $[5Fe_2O_3]$ $[9H_2O]$ (Schwertmann and Taylor, 1989). Ferrihydrite appears as individual spherical particle ranging in size between 2-5 nm. These particles become highly aggregated forming aggregates 100-300 nm in diameter (Shoji et al., 1993).

2.2.6 Chemical characteristics of volcanic soil

Volcanic ash soils display a wide range of chemical characteristics, but only a few of them are important for this project. They are ion exchange equilibrium and adsorption of heavy metal ions.

2.2.6.1 Ion exchange equilibrium

The ion exchange capacity of allophane is not constant and depends on the environmental conditions (Suryaningtyas, 1998). Soils containing allophane, therefore, have values for cation exchange capacities that are strongly depended on the pH and concentrations of leaching solution, the cation in solution and the volume, and nature of the washing media (Shoji et al., 1993).

Shoji et al. (1993) explained the ion exchange features of Andisols as follows: Andisols have cation exchange sites consisting primarily of $-COO^-$ and $\equiv SiO^-$, constant negative charge, and anion exchange sites of $=Al\ (OH)^{2+}$ and $=Fe\ (OH)^{2+}$. The exchangeable cations are commonly Ca^{2+}, Mg^{2+}, K^+, Na^+, Al^{3+}, and the exchangeable anions are Cl^-, NO_3^-, SO_4^{2-}. Characteristics of ion exchange reactions in soil systems are:

(1) ions are retained to the exchange complex through electrostatic attractive forces forming outer-sphere complexes,

(2) the exchange reaction proceeds equivalently and does not disturb charge balance in either the solid or solution phases, and

(3) some ions are preferentially retained by the exchange sites relative to others.

The cation exchange sites of Andisols show a very high selectivity for H^+. Therefore, the soils show no strong acidity, despite their low to very low base saturation. The content of exchangeable bases is generally low in Andisols developed in humid, temperate regions, such as New Zealand, and the base saturation (BS) is less than 50% in subsoils (Suryaningtyas, 1998). The low base content of subsoils is expected since they have less organic matter and lower pH.

2.2.6.2 Sorption of heavy metal ions

Variable charge soils show a very high affinity for heavy metals as compared with constant charge soils (Wada, 1989). The selectivity of heavy metal ions in Andisols typically follows the order: Cd^{2+}, $Co^{2+} < Zn^{2+} < Cu^{2+}$, Pb^{2+}. Shoji et al. (1993) indicated that the reason for this high affinity of metal ions (M) is considered to be due to the high stability of the bidentate surface complexes of allophane and humus as described below:

Heavy metal adsorption results in the release of protons from andisol soil materials. The stoichiometry between proton release and heavy metal sorption has been studied to determine the mechanism of heavy metal sorption. The observed value for the ratio of proton released to divalent heavy metal sorbed is approximately 2 in many cases (Yamamoto, 1982).

The adsorption of heavy metals is affected by pH and the ratio of heavy metal ions to cation exchange capacity. The degree of sorption of heavy metals tends to decrease with decreasing pH values due to proton competition with heavy metals for sorption sites (Wada and Abd-Elfattah, 1978). The selectivity constant tends to decrease with increasing ratios of heavy metal to cation exchange capacity values; maximum sorption

occurs at ratios less than approximately 0.2 (Abd-Elfattah and Wada, 1981).

2.2.7 Physical characteristics of volcanic soil

Volcanic ash soils have many unique physical properties that are attributable directly to the properties of the parent material: the noncrystalline materials formed by weathering, and the soil organic matter accumulated during soil formation (Shoji et al., 1993). These properties include density, porosity, specific surface area, tortuosity and thermodynamic parameters for adsorption-desorption of heavy metal ions on the surface of volcanic ash soils. However, some of these properties are not found in the literature, such as the tortuosity of volcanic ash soil and the adsorption constants for heavy metal ions.

2.2.7.1 Density

Since volcanic ash soils are formed from aggregated particles of some volcanic minerals, they are a porous medium. There are three densities for volcanic ash soils, mineral particle density, aggregate density, and bulk density.

Mineral particle density (ρ_p)

Allophanes in Andisols have particle densities of 2.5 to 2.7 g/cm^3 (Maeda et al., 1977; Bielders et al., 1990), which is similar to the particle density of other mineral soils. Imogolite has a particle density of 2.65 g/cm^3 (Wada and Yoshinaga, 1969).

Aggregate density (ρ_a)

The aggregate density of volcanic ash soil is very important for the development of a model to predict heavy metal ions concentration in the liquid phase in a reactor, because the particulate suspended in liquid is in aggregate form. Its value should be less than mineral particle density (ρ_p) and greater than bulk density (ρ_b), relatively close to the latter. However, no data was found in the literature. If the aggregate of volcanic ash soil could be regarded as a perfect and uniform spherical particulate, the value of aggregate

density (ρ_a) can be calculated through aggregate porosity (ε) and mineral particle density (ρ_p). The formula for calculation of aggregate density is equation (2-38).

Bulk density (ρ_b)

Low bulk density is a characteristic feature of Andisols. Bulk density typical range between 0.4 and 0.8 g/cm^3 in moderately weathered Andisols (Shoji et al., 1993). Allophane is one of the most important noncrystalline materials contributing to the low bulk density of Andisols through the development of porous soil structure. Bulk density is less than 0.9 g/cm^3 when the allophane content is greater than approximately 5%. Gradwell (1974 and 1976) found that the boundary bulk density value that determines whether or not soils are derived from volcanic ash in New Zealand is 0.85 g/cm^3.

Saturated aggregate density (ρ_{as})

In addition to above these densities, saturated aggregate density by liquid (ρ_{as}) is also important. Because the soil aggregates are porous, their intra-pore will be full of liquid in a remediation operation using a batch stirred process, which results in saturated aggregate density (ρ_{as}) being different from aggregate density (ρ_a). Saturated aggregate density differs from aggregate density (ρ_a) just on different fillers within their intra-pore. For aggregate density (ρ_a), air instead of liquid is filled within their intra-pore. Therefore, saturated aggregate density by liquid (ρ_{as}) is greater than aggregate density (ρ_a). Saturated aggregate density (ρ_{as}) can be calculated by equation (2-50).

2.2.7.2 Aggregate porosity (ε)

The porosity and pore size distribution of andisols are dependent on the development of soil structure (Shoji et al., 1993). Young andisols have a greater amount of macropores larger than 100 μm in diameter and a lower amount of micropores (< 0.4 μm) and mesopores (0.4-6.0 μm). In contrast, the moderately weathered andisols have a large amount of micropores (< 0.4 μm) and mesopores (0.4-6.0 μm). The porosity of single-grained sand is about 40 percent while a clayey nonandic soil with an abundance of

crystalline clay minerals shows almost the same porosity based on calculations of equi-size spheres (Shoji et al., 1993). In general, the values of porosity for volcanic ash soil given in literature are of bulk porosity (ε_b) (New Zealand Soil Bureau, 1968). It has the following relation with aggregate porosity (ε), internal porosity and soil packed porosity (ε_e), external porosity:

$$\varepsilon_b = \varepsilon_e + (1-\varepsilon_e)\varepsilon \tag{2-1}$$

The derivation of equation (2-1) is shown in Appendix 5.

2.2.7.3 Aggregate tortuosity (τ)

No data on the tortuosity of volcanic ash soils were found during the literature review. However, there is an inverse ratio relationship between tortuosity and porosity. Several different relationships of these two properties were found from literature. For spherical particles, Brusseau and Rao (1989) and Wakao and Smith (1962) proposed:

$$\tau = \frac{1}{\varepsilon} \tag{2-2}$$

Mackie and Mearres (1955) suggested:

$$\tau = \frac{(2-\varepsilon)^2}{\varepsilon} \tag{2-3}$$

Suzuki and Smith (1972) recommended:

$$\tau = \varepsilon + 1.5(1-\varepsilon) \tag{2-4}$$

Although there have been many different relationships between tortuosity and porosity proposed, Perry and Green (1997) thought that the predictive value of these equations is rather uncertain in general, and vastly different results are obtained from each. However, the first relation above is the most simple.

2.2.7.4 Aggregate size

Measurement or analysis of the aggregate size is difficult because of non-uniform size of the soil aggregates. However, it is a very important model parameter and can not be neglected or replaced by other parameters. In order to reduce or restrict the error from non-uniform aggregate size of volcanic ash soil as much as possible, all samples should be screened by sieves. Removing under size and over size of soil aggregates, the range of soil aggregate size can be defined.

2.2.7.5 Specific surface area

Specific surface area of allophane measurements range from 581 m^2/g by nitrogen at 77 K (Hall et al., 1985) to 700-1100 m^2/g by adsorption of ethylene glycol monoethyl ether (EGME) method on freeze-dried allophane specimens (Egashira and Aomine, 1974) or from 400 to 700 m^2/g in New Zealand soils (Childs and Parfitt, 1987).

Measured surface areas of imogolite range from 700 m^2/g by adsorption of water vapor (Wada and Henmi, 1972) to 900-1000 m^2/g determined by the ethylene glycol monoethyl ether (Egashira and Aomine, 1974). However, electron microscopy indicated that imogolite had a surface area of 1400 to 1500 m^2/g (Wada and Yoshinaga, 1969).

Shoji et al. (1993) indicated that ferrihydrite has a high specific surface area (typically 220 to 560 m^2/g).

2.3. Mathematical model

A mathematical model can easily simulate a process and predict its result, which can save a lot of time and money. Consequently, developing a useful and effective model is significant. No model for predicting the results of leaching heavy metals from volcanic ash soils by water or an organic solvent was found in the literature. However, leaching is important for cleaning soil contaminated with heavy metal ions. Therefore, development

of a model for water or an organic solvent based leaching method would be useful.

2.3.1. Process description

Volcanic ash soil is a heterogeneous material, principally constituting of solid and liquid phases. Therefore, leaching heavy metals from volcanic ash soil by water or an organic solvent is a process of heterogeneous solubilization. Except for the greater complexity of the solid phase and the properties of volcanic ash soil, the process is very similar to adsorbent regeneration by water or cation exchange resin regeneration by inorganic acids. The leaching reagent displaces the adsorbates or cations bound to the solid phase in both processes. Consequently, the solubilization only occurs on the surface of solid particulate. The process is one of fluid-particle mass transfer.

The process of leaching heavy metals from volcanic ash soil by water or an organic solvent will undergo three different stages. The heavy metal concentrations in the liquid phase increases sharply during the initial stage. Then, the rate of solubilizing heavy metal from volcanic ash soil decreases gradually. Finally the heavy metal concentration does not vary with time. Figure 2-1 shows the details (Trefry and Metz, 1984).

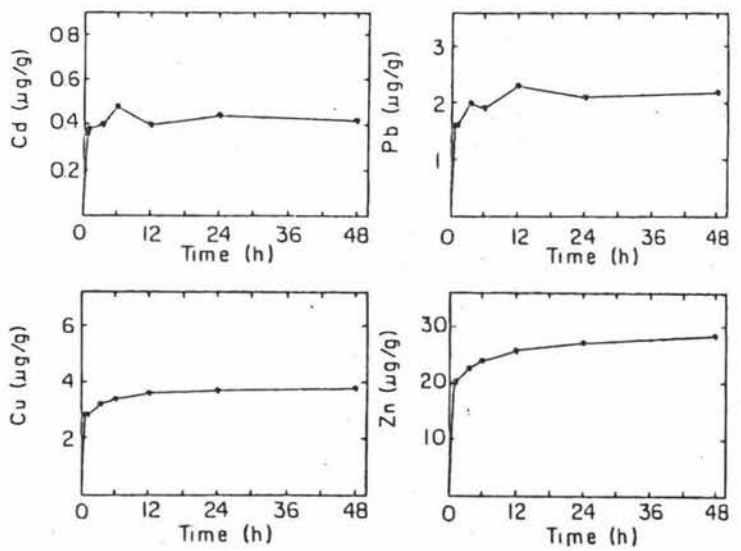

Figure 2-1 Concentrations of Cd, Pb, Cu and Zn vs. time for a leaching process. The aqueous:solid ratio was 51:1. (from Trefry and Metz, 1984)

In the first stage, the process is controlled by interface solubilizing because the resistance of diffusion is not dominant. As the zone of solubilization moves into the interior of the aggregate, the diffusion distance increases and the process is gradually controlled by internal diffusion of adsorbates or organic solvents. Finally, equilibrium is reached, and all parameters do not change with time.

2.3.2. Model selection

Because the aggregates of volcanic ash soil contain large amounts of inert solid materials, solid aggregates remain unchanged in size during leaching. If the process of leaching heavy metals from volcanic soil can be regarded as a special reaction of liquid and solid, two simple idealized models for fluid-particle reactions, the Progressive conversion model (PCM) and the shrinking unleached core model (SUCM), can be used to describe the process. Progressive conversion model is used to describe that the reaction or conversion is continuous and progressive throughout the particle. Figure 2-2 shows the leaching process of a single soil aggregate. Only when the rate of desorption from adsorbent is much slower than that of adsorbate diffusion within adsorbent, the model is suitable. Shrinking unleached core model is used to describe that there exists an unleached core of material, which shrinks in size during leaching, as shown in Figure 2-3. In general, the shrinking unleached core model describes suitably the process that the rate of adsorbate diffusion is greater than that of adsorption or desorption. Therefore, in most cases, the

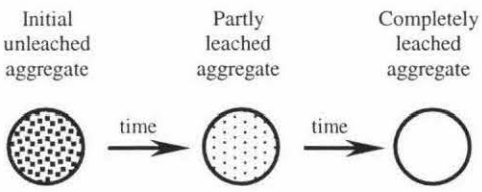

Figure 2-2 According to the progressive conversion model, leaching proceeds continuously throughout the soil aggregate

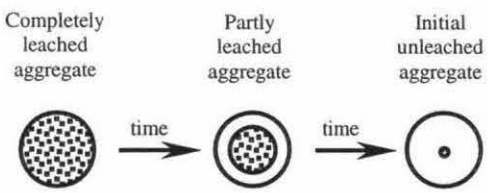

Figure 2-3 According to the shrinking unleached core model, an unleached core of material which shrinks in size during reaction

shrinking unleached core model (SUCM) approximates the real fluid-particle process more closely than does the progressive conversion model (PCM). Heterogeneous leaching occurs first at the outer surface of the volcanic ash soil aggregates. The zone of solubilization then moves into the solid soil aggregate interior, and may leave behind completely treated material and inert solid. Therefore, the shrinking untreated-core model should be selected for this project. It seems to more reasonably represent real particles than does the progressive-conversion model.

In the process of leaching heavy metal from volcanic ash soils by organic solvent, the molecules of organic solvent first transfer through the liquid film from the main body of liquid to the outer surface of the solid soil aggregate, which is called external diffusion. After entering the aggregate they then transfer by diffusion into the zone of solubilization between the untreated and treated part of solid particles, which is internal diffusion. Finally, the molecules of the organic solvent react with the heavy metal ions and dissolve heavy metal ions in the solubilization zone, which is the interface solubilizing process. The heavy metal ions move in the opposite direction. Figure 2-4 shows a sketch of the concentration profile for organic solvent and heavy metal ion, and the sketch of this model. If the leaching process just uses water as leaching reagent, there is not any concentration profile for solvent.

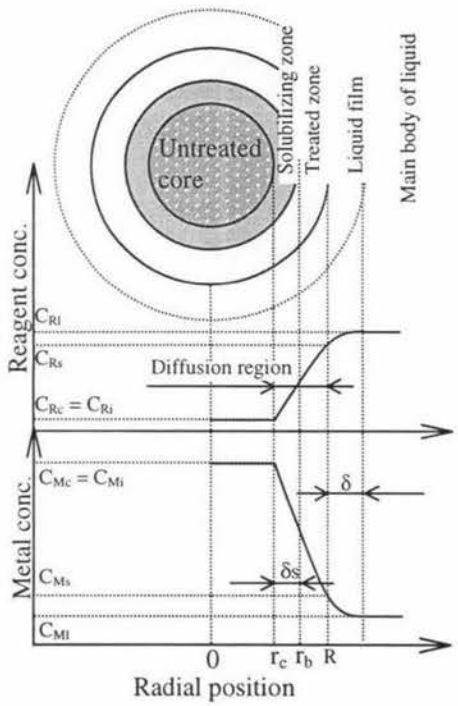

Figure 2-4 Sketch of Untreated-core Model

The faster the rate of solubilizing heavy metal, the thinner the solubilizing zone. If the

rate is very fast, the thickness of solubilizing zone can be treated as zero, which means that the solubilizing zone becomes a solubilizing surface. The overall process of heterogeneous mass transfer contains five steps (Levenspiel, 1972):

① Diffusion of organic solvent molecules through the liquid film surrounding the particle to the outer surface of the solid particle.

② Penetration and diffusion of organic solvent molecules in the pores through the treated zone to the interface of the unreacted core.

③ Reversible solubilizing process of water molecules or organic solvent molecules to heavy metal ions at this interface.

④ Diffusion of heavy metal ions in the pores through the treated zone back to the exterior surface of the solid particle.

⑤ Diffusion of heavy metal ions through the liquid film back into the main body of liquid.

In the five steps, the slowest process will be the rate-controlling step. The overall process rate is determined by the control step. If the rate difference of the five steps is not significant, the overall process rate will be controlled by them simultaneously. In general, all five steps do not occur simultaneously in an actual process. For example, only step 3, 4 and 5 are involved in leaching of heavy metal ions from volcanic soil aggregate just using water as leaching reagent.

2.3.3. Simplifying assumption

Not all characteristics of the process of leaching heavy metals from volcanic ash soils by water or an organic solvent are very important for the process description. Neglecting insignificant factors and idealizing other factors greatly simplifies a model. However, the insignificant factors are different for each process, so they need to be identified carefully.

2.3.3.1 Constant aggregate size

In this study, in order to express and describe the process conveniently by means of

mathematics, the soil aggregate size is treated as uniform and constant. In general, the aggregate does not shrink with solubilization of heavy metals from the surface of volcanic materials, thus the use of the shrinking aggregate model is not appropriate. The structure of soil aggregates is unlikely to change in the leaching process.

2.3.3.2 Constant temperature

The use of water or organic solvent for leaching of heavy metals from volcanic ash soil is a process of dissolution, in which water or organic solvent solubilizes heavy metal ions bound to the solids of volcanic ash soil. For the process, the heat of solution is quite low, and the content of heavy metals in volcanic ash soil is not high enough to lead to a change in temperature due to solubilization, so the process can be regarded as a constant temperature process.

2.3.3.3 Spherical aggregates

The aggregates of volcanic ash soil are mainly constituted of organic matter and mineral particles. Because they were formed from the weathering of tephras or pyroclastic materials, not all aggregates of volcanic ash soil are spherical. Consequently, a sphericity factor may be needed to correct the results based on spherical aggregate. However, this factor is usually difficult to obtain and varies from soil to soil. Therefore, an assumption that the aggregates are spherical is necessary. In addition, all aggregates are assumed to have a smooth exterior surface. Since the aggregate size of volcanic ash soil is small enough, the physical properties of volcanic ash soil are not obviously different in any direction. This means that the aggregates of volcanic ash soils can be regarded as being isotropic spherical aggregates.

2.3.4. Mathematical expression

In the process of leaching heavy metal from volcanic ash soil, the leaching reagent used may be water or an organic solvent. For economic considerations, the aqueous

solution of an organic solvent instead of the pure solvent is used in most cases. Therefore, the concentration distribution of the leaching reagent may be different for water and organic solvent because water is a pure substance and its concentration can be regarded as a constant but organic solvent may be not if its aqueous solution instead of itself is used. Thus, mathematical expressions for water leaching and organic solvent leaching are different.

There may be three potential control steps for the overall process rate. They are external diffusion, internal diffusion and solubility at the interface. They can determine the overall process rate either individually or in combination, depending on the rates of the individual process components.

2.3.4.1 External diffusion control

External diffusion control is also called film diffusion control. Under film diffusion control, the mass transfer resistance of the liquid film is very close to that of the overall process, and other resistances can be neglected. Therefore, the overall process rate can be treated in terms of the transfer rate of the liquid film. If the process can not be treated as a steady-state process, then Fick's second law needs to be used for describing the process. For a spherical soil aggregate, the liquid film around it is a spherical shell. Therefore, one dimensional form of Fick's second law should be suitable. The diffusion model describing mass transfer within a spherical liquid droplet with non-constant diffusion coefficient can be used.

Because there is only a single phase in liquid film, the diffusion of heavy metal ions and organic solvent molecules within the liquid film is homogenous mass transfer. Coulson and Richardson (1977) derived a partial differential equation of second level to describe the mass transfer process. For heavy metal ion, the concentration distribution can be expressed by following equation:

$$\frac{\partial C_M}{\partial t} = \frac{\partial}{\partial r}\left(D_{IM}\frac{\partial C_M}{\partial r}\right) + \frac{2D_{IM}}{r}\frac{\partial C_M}{\partial r} \qquad \text{for } R \le r \le R+\delta \qquad (2\text{-}5)$$

where t is time (s); D_{lM} is the diffusion coefficient in the liquid phase for heavy metal ions (m^2/s); C_M is the concentrations of heavy metal ion (mol/m^3); r is the distance from the centre to arbitrary surface of particle interior (m); R is the radius of aggregate (m); δ is the thickness of liquid film (m). The derivation of above equations is shown in Appendix 1.

Since the liquid film is very thin, the steady-state process is established very quickly. After it becomes a steady-state process, Fick's first law is suitable for describing the process. Under steady state conditions, equation (2-5) becomes:

$$0 = \frac{\partial}{\partial r}(D_{IM}\frac{\partial C_M}{\partial r}) + \frac{2D_{IM}}{r}\frac{\partial C_M}{\partial r} \tag{2-6}$$

Separating variables and integrating, above equation changes to:

$$\ln(D_{IM}\frac{\partial C_M}{\partial r}) = -2\ln r + c'' \tag{2-7}$$

The following equation can be obtained by arranging equation (2-7):

$$c' = r^2 D_{IM}\frac{\partial C_M}{\partial r} \tag{2-8}$$

where c'' and c' are integral constants. Above equation multiplied by 4π, then it becomes:

$$4\pi c' = 4\pi r^2 D_{IM}\frac{\partial C_M}{\partial r} \tag{2-9}$$

Equation (2-9) can calculate the amount of mass transfer through spherical surface $4\pi r^2$. If it is divided by $4\pi R^2$, Fick's first law based on the exterior surface of a single solid particle can be obtained:

$$\nu_M = -\frac{1}{4\pi R^2}\frac{dn_M}{dt} = -\frac{4\pi r^2}{4\pi R^2}D_{IM}\frac{dC_M}{dr} \tag{2-10}$$

where ν_M is the mass transfer flux of heavy metal ion based on exterior surface of single

solid particle (mol/m^{2}s); n_M is the number of moles of heavy metal ion (mol).

If the diffusion coefficient (D_{lM}) is constant, the form of integral for equation (2-10) is:

$$v_M = -\frac{D_{lM}}{\delta}(C_M|_{R+\delta} - C_M|_R) \qquad (2\text{-}11)$$

where R is the radius of soil aggregate (m) and δ is the thickness of liquid film (m). Because δ is difficult to measure, k_{lM} is often used and can be expressed:

$$k_{lM} = \frac{D_{lM}}{\delta} \qquad (2\text{-}12)$$

where k_{lM} is the corresponding mass transfer coefficient of heavy metal ions in liquid film (m/s). The detailed derivation of these equations is shown in Appendix 1.

In general, the liquid film is seldom limiting in the leaching of heavy metals from volcanic ash soil because continuously and turbulently stirring makes sure to reduce greatly the thickness of fluid boundary film and its control of the overall process.

2.3.4.2 Internal diffusion control

Internal diffusion is defined as intra-particle transport. It actually may involve two mass transfer processes, pore and surface diffusion which act in parallel. Generally only the more rapid of the two needs to be considered in describing adsorption rates (Slejko, 1985).

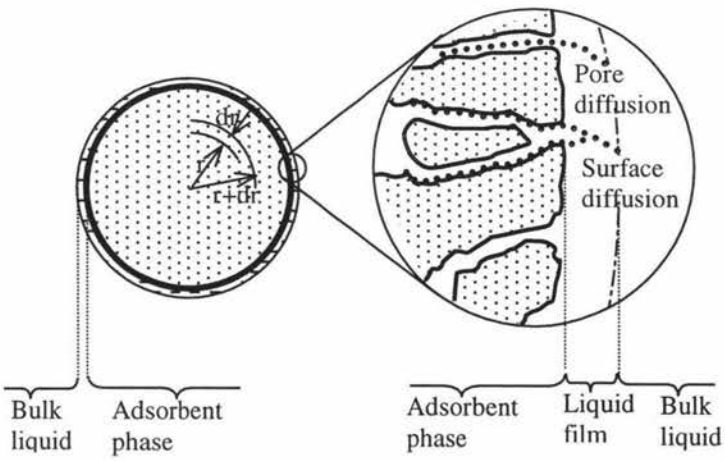

Figure 2-5 Mass transport mechanism in a soil aggregate

The surface diffusion model assumes that the adsorbate firstly is adsorbed onto the wall of the pores, and then diffuses along the surface of the pores. Treybal (1980) indicated that surface diffusion was a phenomenon accompanying adsorption of solute onto the surface of the pores of the solid. Therefore, surface diffusion only occurs in physical adsorption process, and it does not exist individually. There is no surface diffusion in some surface processes of non-accumulation, such as ion exchange and fluid-solid catalytic reaction process. In addition, surface diffusion does not occur in a chemical adsorption process either because the chemical bond between adsorbent and adsorbate is too strong to break. Figure 2-5 shows the sketch of surface diffusion. Surface diffusion can be described by a two-dimensional analog of Fick's law, with surface concentration expressed (Treybal, 1980).

In the pore diffusion model, it is assumed that the adsorbate diffuses via the pores of the solid particle interior and is taken up by adsorption onto the wall of the pores, as shown in Figure 2-5. Pore diffusion is more common, and it can occur in physical or chemical adsorption process because it is independent of surface accumulation.

In the case of internal diffusion control, the solubilizing zone does not spread over the whole diffusion range, which means that the thickness of the solubilizing zone is less than the radius of the soil aggregate. Therefore, the solubilizing zone must move with time from the surface to the interior of the solid particle. The region at the head of the solubilizing zone is the unreacted core. Consequently, the assumption that the thichness of the solubilizing zone in unreacted core model is stationary is reasonable (Levenspiel, 1972).

(1) Pore diffusion domination

The process is controlled by pore diffusion if the pore diffusion flux is much greater than surface diffusion flux. The surface diffusion can be neglected in this case. If the process is in unsteady-state, the descriptive equation can be derived from material balance at any internal region of soil aggregates. The details are shown in Chapter 4.

If only water is used as a leaching reagent, the mathematical expression of the concentration distribution for heavy metal ions is:

$$\frac{\partial C_M}{\partial t}+\frac{\rho_{as}}{\varepsilon}\frac{\partial q_M}{\partial t}=\frac{\partial}{\partial r}(D_{eM}\frac{\partial C_M}{\partial r})+\frac{2D_{eM}}{r}\frac{\partial C_M}{\partial r} \quad \text{for } r_c \le r \le R \tag{2-13}$$

where D_{eM} is the effective diffusion the coefficient for heavy metal ion (m^2/s); r_c is the distance from the centre to the surface of the untreated core (m). C_M is the intra-aggregate concentration of heavy metal ion (mol/m^3); ε is the porosity of aggregate. ρ_{as} is the density of soil aggregate saturated by liquid (kg/m^3); q_M is the amount of heavy metal ions adsorbed on the surface of intra-aggregate (mol/kg).

Under the steady-state situation, the diffusion rate in the pore is:

$$v_M=-\frac{1}{4\pi R^2}\frac{dn_M}{dt}=-\frac{4\pi r^2}{4\pi R^2}D_{eM}\frac{dC_M}{dr} \tag{2-14}$$

If D_{eM} is independent from the concentration, equation (2-14) becomes:

$$v_M=-\frac{r_c}{R}\cdot\frac{D_{eM}}{R-r_c}(C_M|_R-C_M|_{r_c}) \tag{2-15}$$

(2) Surface diffusion domination

Surface diffusion will dominate if the pore diffusion flux is very small. In this case, surface diffusion flux approximates the overall internal diffusion flux. If only water is used as a leaching reagent for an unsteady-state system, the following partial differential equation can be used to describe the concentration distribution of heavy metal ion:

$$\frac{\partial q_M}{\partial t}+\frac{\varepsilon}{\rho_{as}}\frac{\partial C_M}{\partial t}=\frac{\partial}{\partial r}(D_{sM}\frac{\partial q_M}{\partial r})+\frac{2D_{sM}}{r}\frac{\partial q_M}{\partial r} \quad \text{for } r_c \le r \le R \tag{2-16}$$

where D_{sM} is the surface diffusion coefficient for the heavy metal ion (m^2/s). The derivation is shown in Chapter 4.

Under the steady-state situation, the diffusion rate at the surface is:

$$v_{sM} = -\frac{1}{4\pi R^2}\frac{dn_{sM}}{dt} = -\frac{4\pi r^2}{4\pi R^2} D_{sM}\frac{dq_M}{dr} \qquad (2\text{-}17)$$

where v_{sM} is the surface mass transfer flux of heavy metal ion based on the external surface of single solid particle [m(mol/kgs)]. There is the following relation between v_{sM} and v_M:

$$v_M = \frac{\rho_{as}}{\varepsilon} v_{sM} \qquad (2\text{-}18)$$

If D_{sM} is independent of q_M, the integral form of equation (2-17) is:

$$v_{sM} = -\frac{r_c}{R}\cdot\frac{D_{sM}}{R - r_c}(q_M|_R - q_M|_{r_c}) \qquad (2\text{-}19)$$

(3) Parallel pore and surface diffusion

If the difference between pore diffusion flux and surface diffusion flux is small, neither can be neglected. If the process is unsteady-state and only water is the leaching reagent, the partial differential equation describing the concentration distribution of heavy metal ion is:

$$\varepsilon\frac{\partial C_M}{\partial t} + \rho_{as}\frac{\partial q_M}{\partial t} = \frac{1}{r^2}\frac{\partial}{\partial r}[r^2(\varepsilon D_{eM}\frac{\partial C_M}{\partial r} + \rho_{as} D_{sM}\frac{\partial q_M}{\partial r})] \quad \text{for } r_c < r < R \qquad (2\text{-}20)$$

The derivation of the above equations is shown in Chapter 4. If the process is steady state, the internal diffusion rate is:

$$v_{sM} = \frac{1}{4\pi R^2}\frac{dn_M}{dt} = -\frac{4\pi r^2}{4\pi R^2}(\frac{\varepsilon}{\rho_{as}} D_{eM}\frac{dC_M}{dr} + D_{sM}\frac{dq_M}{dr}) \qquad (2\text{-}21)$$

If D_{eM} and D_{sM} are constant, the integrated form of equation (2-21) is:

$$v_{sM} = \frac{\varepsilon}{\rho_{as}}\frac{r_c}{R}\frac{D_{eM}}{R - r_c}(C_M|_R - C_M|_{r_c}) + \frac{r_c}{R}\frac{D_{sM}}{R - r_c}(q_M|_R - q_M|_{r_c}) \qquad (2\text{-}22)$$

In general, pore diffusion is the dominant mechanism for internal diffusion, but surface diffusion is not negligible if the adsorption amount of adsorbate is large (Noll et al., 1992). However, the surface diffusion coefficient is not easy to obtain.

2.3.4.3 Interface solubilizing control

If the rate of solubilizing of heavy metal ions is slower than the rate of diffusion in the aggregate interior, the thickness of the solubilizing zone is greater than zero. The slower the solubilization rate, the thicker the solubilizing zone (Levenspiel, 1972). In the case of interface solubilizing control, the solubilizing zone may spread to the whole radius of soil aggregate. In the solubilizing zone, diffusion and solubilization occur simultaneously. The kinetic equation for heavy metal ion diffusion is:

$$v_M = \frac{1}{4\pi R^2}\frac{dn_M}{dt} = -k_{sM}(C_{lM} - C_{sM}) \qquad (2\text{-}23)$$

where k_{sM} is the first order rate constants for the solubilization of heavy metal ion (m/s), and subscript l and s represent liquid phase and internal surface of intra-aggregate of volcanic ash soil, respectively.

2.3.4.4 Combination control

If there is no single rate controlling step in the process, the process is controlled by all the relevant steps. Under unsteady-state condition for heavy metal ion, the describing equations have the following form:

$$\begin{cases} \dfrac{\partial C_M}{\partial t} = \dfrac{\partial}{\partial r}(D_{lM}\dfrac{\partial C_M}{\partial r}) + \dfrac{2D_{lM}}{r}\dfrac{\partial C_M}{\partial r} & \text{for } R < r \le R+\delta \\ \varepsilon\dfrac{\partial C_M}{\partial t} + \rho_{as}\dfrac{\partial q_M}{\partial t} = \dfrac{1}{r^2}\dfrac{\partial}{\partial r}[r^2(\varepsilon D_{eM}\dfrac{\partial C_M}{\partial r} + \rho_{as}D_{sM}\dfrac{\partial q_M}{\partial r})] & \text{for } r_b < r < R \\ \dfrac{1}{4\pi R^2}\dfrac{\partial n_M}{\partial t} = -k_{sM}(C_{lM} - C_{sM}) & \text{for } r_c < r < r_b \\ C_M = C_{Mi} & \text{for } 0 \le r < r_c \end{cases} \qquad (2\text{-}24)$$

where C_{Mi} is the initial concentration of heavy metal ion (mol/m^3).

The following equation may be used to describe the overall process under steady-state situation:

$$v_M = \frac{1}{4\pi R^2}\frac{dn_M}{dt} = -\frac{C_{lM} - \frac{k_{s1}}{k_{s2}}C_{sM}}{\frac{1}{k_{lM}} + \frac{R(R-r_c)}{r_c D_{eM}} + \frac{R^2}{r_c^2 k_{s2}}} \qquad (2\text{-}25)$$

2.3.5. Parameters for the model

Some parameters for the process of leaching heavy metals from volcanic ash soil by an organic reagent can be calculated from an appropriate empirical model from the literature. Nevertheless, some parameters can only be obtained from experiments.

2.3.5.1. Diffusion coefficient

There are two different diffusion mechanisms as solute diffuses through a porous medium. They are pore diffusion and surface diffusion. Pore diffusion consists of molecular diffusion and Knudsen diffusion for which collisions between molecules in fluid phase are much less numerous than those between molecule and pore wall. The molecular mean free path of liquids is very small, and Knudsen diffusion can be neglected. However, the influence of the pores in the aggregates of volcanic ash soil on the diffusion process can not be neglected. Therefore, the calculations of the external diffusion coefficient and the pore diffusion coefficients should be independent from each other.

2.3.5.1.1 External diffusion coefficient

External diffusion is defined as the diffusion through a liquid film, and it is molecular diffusion. A salt such as sodium chloride (NaCl) dissociates in solution, ions rather than

molecules diffuse since it is a strong electrolyte and it will ionise completely in water. In general, ionic diffusion coefficients are much greater than molecular diffusion coefficients. However, ionic diffusion does not change electric neutrality of the solution if no external electric field is applied to the solution, which means cationic or anionic diffusion always is bound by the opposite charge ionic diffusion. Therefore, the diffusion of a single salt in water can be treated as a molecular diffusion (Reid et al., 1987). The theory of diffusion of salts at low concentration is well developed. The Nernst-Haskell equation describes the limiting diffusion coefficient of a single salt:

$$D^0_{IM} = \frac{RT}{F^2} \frac{\left(\left|\frac{1}{n_+}\right| + \left|\frac{1}{n_-}\right|\right)}{\left(\frac{1}{\lambda^0_+} + \frac{1}{\lambda^0_-}\right)} \qquad (2\text{-}26)$$

where n_+ and n_- are valences of cation and anion, respectively; λ^0_+ and λ^0_- are the limiting (zero-concentration) ionic conductance of cation and anion, respectively [$(A/cm^2)\cdot(V/cm)\cdot(g\ equivalent/cm^3)$]; T is absolute temperature (K); R is gas constant (8.314J/mol·K); F is Faraday constant (96,500 C/g equivalent).

The values of the limiting ionic conductance of cation and anion, λ^0_+ and λ^0_-, at 25°C, respectively was listed in Table 2-3 (Harned and Owen, 1950).

Table 2-3 Ionic conductances in water at 25 °C

Cation	λ^0_+	Anion	λ^0_-
H^+	349.8	Cl^-	76.3
$\frac{1}{2} Mg^{+2}$	53.1	HCO_3^-	44.5
$\frac{1}{2} Ca^{+2}$	59.5	NO_3^-	71.4
$\frac{1}{2} Cu^{+2}$	54.0	$\frac{1}{2} SO_4^{-2}$	80.0
$\frac{1}{2} Zn^{+2}$	53.0		

From Reid et al. (1987)

As the salt concentration becomes finite and increases, the diffusion coefficient

eases rapidly and then usually rises, often becoming greater than D^0 at high normality. re 2-6 illustrates the typical trend for three simple salts (Reid et al., 1987).

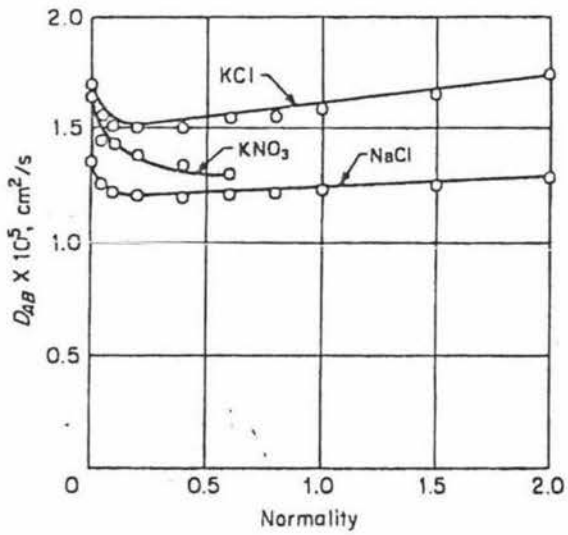

gure 2-6 Effect of concentration on diffusivity of electrolytes in aqueous solution at 18.5 °C. Solid lines calculated by using Eq (2-38). (Reid et al., 1987)

nitial decrease at low concentrations is proportional to the square root of the ıtration, but deviations from this trend are usually significant above 0.1 N (Reid et '87). Gordon (1937) proposed an empirical equation that could be applied to a ı at concentrations up to 2 N:

$$D_{IM} = D^0_{IM} \frac{\mu_s}{\mu} \frac{1}{C_s \overline{V}_s} \left(1 + \frac{\partial \ln \gamma_\pm}{\partial \ln m}\right) \qquad (2\text{-}27)$$

μ_s is the viscosity of the solvent and μ is the viscosity of the solution ($P_a s$); C_s is the :oncentration of the solvent (mol/m³); $\overline{V}_s$ is the partial molar volume of the solvent l); $\gamma_\pm$ is mean ionic activity coefficient of the solute; and m is the molality of the mol/kg solvent) (Reid et al., 1987). The relationship between molality and molarity

$$m = \frac{1}{\frac{\rho_l}{C} - M_t} \qquad (2\text{-}28)$$

where ρ_l is density of the liquid or solution (kg/m^3); C is the molarity of solute (mol/m^3); and M_t is the molecular weight of solute (kg/mol). The derivation of the above relationship is shown in Appendix 2.

In many cases, the product of $C_s \overline{V}_s$ is close to unity, as is the viscosity ratio μ_s/μ, so that Gordon's relation provides an activity correction to the diffusion coefficient at infinite dilution. Lobo (1984) tabulated $\gamma_\pm$ as a function of m for many aqueous solutions. Bromley (1973) presents an analytical relation:

$$\ln \gamma_\pm = |n_+ \cdot n_-| \cdot \ln 10 \cdot [\frac{-0.511\sqrt{I}}{1+\sqrt{I}} + \frac{(0.06+0.6B)\cdot I}{(1+\frac{1.5}{|n_+ \cdot n_-|} I)^2} + \frac{B \cdot I}{|n_+ \cdot n_-|}] \qquad (2\text{-}29)$$

where I is the mean ionic strength (mol/kg) and it can be calculated by the following equation:

$$I = \frac{\sum m_i \varphi_i n_i^2}{2} \qquad (2\text{-}30)$$

where φ_i is the stoichiometric number of ions in the salt molecule. B is a constant for each salt (kg/mol) and its value for many salts is listed in Table 2-4 (Bromley 1973).

Table 2-4 B values of some salts at 25 °C

1-1 salts	**B Kg/mol**	**1-2 salts**	**B Kg/mol**	**1-3 salts**	**B Kg/mol**	**2-1 salts**	**B Kg/mol**
$AgNO_3$	-0.0828	Na_2CO_3	0.0089	K_3PO_4	0.0344	$BaCl_2$	0.0638
NaCl	0.0547	K_2SO_4	-0.0320	Na_3AsO_4	0.0159	$Zn(NO_3)_2$	0.1002
2-2 salts	**B Kg/mol**	**3-1 salts**	**B Kg/mol**	**3-2 salts**	**B Kg/mol**	**4-1 salts**	**B Kg/mol**
$CuSO_4$	-0.0364	$AlCl_3$	0.1089	$Al_2(SO_4)_3$	-0.0044	$ThCl_4$	0.1132
$CdSO_4$	-0.0371	$Cr(NO_3)_3$	0.0919	$Cr_2(SO_4)_3$	0.0122	$Th(NO_3)_4$	0.0894

From Bromley (1973).

If the solution just contains only single salt, m_i is the same for cation and anion. Therefore, equation (2-30) become the following:

$$I = \frac{m \sum \varphi_i n_i}{2} \qquad (2\text{-}31)$$

Because the liquid concentration of heavy metal ions is almost always less than 200 ppm, the volume of solution should be very close to that of the solvent. Consequently, the volume of the solvent can be regarded as the volume of the solution. Thus, the density of the solution becomes a linear function of molarity of solute:

$$\rho_l = \rho_s + M_t \cdot C \tag{2-32}$$

where ρ_s is the density of solvent (kg/m^3). Substitute equation (2-32) into equation (2-28) and we can get:

$$m = \frac{C}{\rho_s} \tag{2-33}$$

Therefore, equations (2-27) and (2-30) become respectively:

$$D_{lM} = D_{lM}^0 \frac{\mu_s}{\mu} \frac{1}{C_s \overline{V}_s} \left(1 + \frac{\partial \ln \gamma_{\pm}}{\partial \ln C}\right) \tag{2-34}$$

$$I = \frac{\sum \frac{C_i}{\rho_s} \varphi_i n_i^2}{2} = \frac{C}{\rho_s} \frac{\sum \varphi_i n_i^2}{2} \tag{2-35}$$

The derivation of the above relationships is shown in Appendix 3.

The diffusion coefficient of a salt in aqueous solution calculated by the above formula is reliable only at 25 °C because all values of these parameters in the formula are for 25 °C. Reid et al., (1987) indicated that the calculated results for other temperatures need to be corrected by the following equation:

$$D_t = D_{25} \frac{T}{298} \frac{\mu_{25}}{\mu} \frac{\mu_s}{\mu_{s25}} \frac{\rho_{s25} \overline{V}_{s25}}{\rho_s \overline{V}_s} \tag{2-36}$$

where D_{25} and D_t are the diffusion coefficients at 25 °C and another temperature (m^2/s), respectively; μ_{25} and μ_{s25} are the viscosities of solution and solvent at 25 °C ($P_a s$),

respectively; ρ_{s25} is the density of solvent at 25 °C (kg/m^3); and $\overline{V}_{s25}$ is the partial molar volume of solvent at 25 °C (m^3/mol).

2.3.5.1.2 Pore diffusion coefficient

Shoji et al. (1993) indicated that volcanic ash soil is porous and the mean pore radius was about 30Å (1Å = 10^{-10} m). Because of the effect of pores, the resistance to diffusion in the aggregate of volcanic ash soil is greater than that in bulk liquid. Therefore, the effective diffusion coefficient rather than the molecular diffusion coefficient should be used for diffusion in porous media. The following is an equation for the effective diffusion coefficient (Coulson and Richardson, 1979; Perry and Green, 1997):

$$D_e = \frac{\varepsilon}{\tau} D_l \qquad (2\text{-}37)$$

where τ is the tortuosity factor; ε is the internal void fraction of the soil aggregate; and D_l is the molecular diffusion coefficient (m^2/s). According to the definition of the porosity (ε), it can be calculated by following equation:

$$\varepsilon = \frac{\rho_p - \rho}{\rho_p} \qquad (2\text{-}38)$$

where ρ_p is the density of mineral particle of volcanic ash soil (kg/m^3); and ρ is the dry aggregate density of volcanic ash soil (kg/m^3).

However, the value of the dry aggregate density of volcanic ash soils (ρ) is difficult to obtain, but it has the following relationship to the densities of mineral particle and bulk volcanic ash soil:

$$\rho_b < \rho < \rho_p \qquad (2\text{-}39)$$

where ρ_b is the density of dry bulk volcanic ash soil (kg/m^3). If the aggregate size of

volcanic ash soil is very small, the intra-aggregate and inter-aggregate pore sizes are very close to each other. Thus, the density of the dry soil aggregate (ρ) will approximate the density of dry bulk soil (ρ_b). The typical particle density of volcanic ash soil (ρ_p) is quoted as 2.5 – 2.7 g/cm^3, and the typical bulk density of volcanic ash soil is 0.85 g/cm^3 (Shoji et al., 1993). The dry bulk density of volcanic ash soils of the Mountain Egmont region of the North Island, New Zealand, is 0.74 g/cm^3 (New Zealand Soil Bureau, 1968).

2.3.5.1.3 Surface diffusion coefficient

The surface diffusion coefficient for electrolytes in aqueous solution is not found in the literature, only those for a few gases are available. In addition, no means of estimation of the surface diffusion coefficient is reported. Therefore, omitting surface diffusion is necessary. However, that may lead to decreasing accuracy of the results predicted by the model, because there are not any reasons to justify this omission.

2.3.5.1.4 Overall diffusion coefficient

Applying the principle of series resistance addition and ignoring the resistance of surface diffusion, the overall diffusion coefficient can be calculated by the following approximate equation:

$$D_T \approx \frac{1}{\frac{1}{D_l} + \frac{1}{D_e}} \qquad (2\text{-}40)$$

2.3.5.2 Mass transfer coefficient

Levins and Glastonbury (1972a and b) studied a transfer-controlled mass transfer to particles suspended in a stirred vessel which means that non-transfer-controlled steps, including surface chemical reaction, and adsorption and desorption equilibrium in heterogeneous chemical reaction process, are much faster than that of transfer-controlled steps, and proposed a formula of calculation for mass transfer for this process:

$$Sh = 2 + 0.44\,Re^{0.5}\,Sc^{0.38} \tag{2-41}$$

Sh is the Sherwood number and its definition is:

$$Sh = \frac{k_l \cdot d_p}{D_l} \tag{2-42}$$

where k_l is the mass transfer coefficient in the liquid phase (m/s); d_p is diameter of the suspended particle (m); and D_l is the liquid diffusion coefficient (m^2/s). Sc is the Schmidt number and it can be described by the following formula:

$$Sc = \frac{\nu}{D_l} = \frac{\mu}{D_l \rho_l} \tag{2-43}$$

where ν is kinematic viscosity of the solution (m^2/s). R_e is Reynolds number and it was defined as:

$$R_e = \frac{d_p \cdot \upsilon}{\nu} = \frac{d_p \upsilon \rho_l}{\mu} \tag{2-44}$$

where υ is the resultant relative velocity (m/s) which was defined as (Levins and Glastonbury, 1972b):

$$\upsilon = \sqrt{u_E^{\,2} + u_t^{\,2} + u_s^{\,2}} \tag{2-45}$$

where u_E is effective relative velocity for mass transfer to neutral density particles (m/s); u_t is terminal velocity (m/s); and u_s is the slip velocity arising from differences in inertia between particles and liquid (m/s). Levins and Glastonbury (1972b) proposed the following:

$$u_E = 0.93 \frac{\nu}{d_p} \left(\frac{d_p^{\frac{4}{3}} \cdot \zeta^{\frac{1}{3}}}{\nu} \right)^{1.23} \cdot \left(\frac{D_s}{D_T} \right)^{0.35} \tag{2-46}$$

where D_s and D_T are diameters of stirrer and tank (m), respectively; ζ is the energy dissipation rate unit mass of fluid (J/kg).

$$\zeta = \frac{P}{V_l \rho_l} \tag{2-47}$$

where P is input energy (J/s); V_l is the volume of liquid (m^3).

$$P = 60^3 \rho_l N^3 \cdot D_s{}^5 P_o \tag{2-48}$$

where N is stirrer speed (r/min); P_o is an energy number.

$$u_t = \sqrt{\frac{4g \cdot d_p(\rho_{as} - \rho_l)}{3\rho_l C_D}} \tag{2-49}$$

where ρ_{as} is the density of aggregate of volcanic ash soil saturated by liquid (kg/m^3); C_D is drag coefficient (dimensionless). The saturated aggregate density can be calculated by the following formula:

$$\rho_{as} = (1-\varepsilon)\rho_p + \varepsilon\rho_l \tag{2-50}$$

The derivation of equation (2-50) is shown in Appendix 4. C_D can be calculated by following equations (Perry and Green, 1997):

$$\begin{cases} C_D = \dfrac{24}{R_e} & R_e < 0.1 \\ C_D = \dfrac{24}{R_e}(1 + 0.14 R_e{}^{0.70}) & 0.1 < R_e < 1000 \\ C_D = 0.445 & 1000 < R_e < 350000 \\ C_D = 0.19 - \dfrac{8\times10^4}{R_e} & R_e > 10^6 \end{cases} \tag{2-51}$$

$$u_s = b \cdot (\rho_{as} - \rho_l)^a \tag{2-52}$$

where both a and b are functions of the diameter of solid particles. The relationship between the diameter of solid particles and the functions can be obtained from Levins and Glastonbury (1972a).

The terminal velocity (u_t) is a axial velocity, and the effective relative velocity (u_E) is a circular velocity, so that the slip velocity (u_s) must be a radial velocity. The details are shown in Figure 2-7.

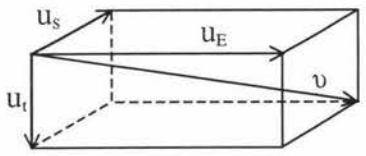

Figure 2-7 The relation of the three velocities

2.3.5.3 Specific surface area

Studies on specific surface area for volcanic ash soil (allophane) produced results of 581 m^2/g (Egashira and Aomine, 1974); 700–1100 m^2/g (Hall et al., 1985); and 400–700 m^2/g (Childs and Parfitt, 1987). The data for other types of volcanic ash soils can be obtained from (Shoji et al., 1993).

2.3.6. Equilibrium model and its parameters

Volcanic ash soil has a large specific surface area, so the amount of heavy metal adsorbed by volcanic ash soil will increase with the industrial use of heavy metals, and can not be neglected. The first and most important characterisation of volcanic soil-heavy metal interaction due to adsorption is in terms of equilibrium behaviour.

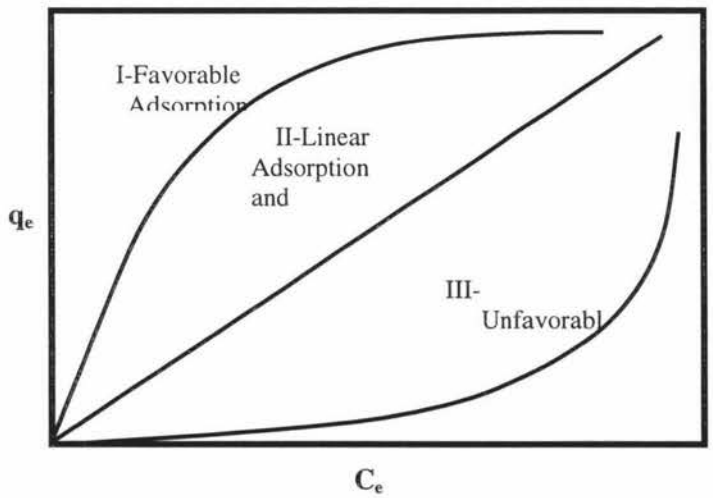

Figure 2-8 Types of equilibrium sorption separations: q_e = amount sorbed and C_e = amount in solution (Weber, 1972).

An equilibrium relationship is obtained by plotting the amount of heavy metal adsorbed per unit mass of adsorbent *versus* the solution phase concentration at constant temperature under equilibrium conditions. Phenomenological differences among adsorption processes are illustrated graphically by the phase partitioning relationships shown in Figure 2-8 (Weber, 1972). The favourable adsorption is the most common among the three different equilibrium patterns. Some of models frequently used to describe equilibrium patterns of heavy metal in solid adsorbents are described below.

2.3.6.1 Linear model

The simplest adsorption isotherm, in which the amount adsorbed is directly proportional to the equilibrium concentration, is often referred to as Henry's law:

$$q_M = KC_M \tag{2-53}$$

where q_M is adsorption amount of adsorbate (mg/g); C_M is equilibrium concentration of metals in liquid (mg/l); K is an isotherm constant. In these systems the adsorbed layer is extremely dilute.

2.3.6.2 Langmuir model

The isotherm model was developed by Langmiur (1918) to describe the adsorption of gases onto solids. The model is based on the assumptions that adsorption is as monomolecular layer and the energy of adsorption for each molecule is the same. With these assumptions, the model can be derived from a rate balance. The commonly quoted form is:

$$q_M = \frac{Q_0 b C_M}{1 + b C_M} \tag{2-54}$$

where Q_0 is a temperature-independent constant which is supposed to represent a fixed number of surface sites; b is a temperature dependent equilibrium constant related to the

heat of adsorption, and follows a vant-Hoff equation:

$$b = b_0 e^{-\frac{\Delta H}{RT}} \tag{2-55}$$

where ΔH is the heat of adsorption (kJ), b_0 is the nature of a frequency factor (Noll et al., 1992).

2.3.6.3 BET model

In 1938, Brunauer, Emmett, and Teller showed how to extend Langmuir's approach to multilayer adsorption, and their equation has come to be known as BET equation. The basic assumptions of the BET equation are that any given layer need not be complete before subsequent layers can form, and that the first layer of molecules adhere to the surface with an energy comparable to the heat of adsorption for monolayer attachment, and that subsequent layers are essentially condensation reactions (Slejko, 1985). The BET equation takes the form:

$$q_M = \frac{BC_M Q_0}{(C_M - C_s)[1+(B-1)\frac{C_M}{C_s}]} \tag{2-56}$$

where C_s is the saturation concentration (solubility limit) of the solute; B is a constant expressive of the energy of adsorption.

Because of the assumption of condensation for the second and subsequent layer, the BET equation is only suitable for adsorption of gas-solid system. For a liquid-solid system, the BET model is not satisfying.

2.3.6.4 Gibbs model

The model was developed by Gibbs in 1876. A thermodynamic balance was achieved between two phases. Most nonpolar substances tend to reduce the interfacial tension of

water by accumulating at a phase boundary and increasing the area of the interface (Weber, 1972). The Gibbs equation has the form:

$$\Gamma = -\frac{C_M}{RT}\frac{d\gamma}{dC_M} \qquad (2\text{-}57)$$

where Γ is the surface excess (amount of material adsorbed at the surface in excess of that existing in the bulk phase); γ is the surface tension. The model is used infrequently in practice because most of the fundamental assumptions involved in development of the model do not apply to a practical situation.

2.3.6.5 Freundlich model

Despite the sound theoretical basis of the Langmuir, BET and Gibbs models, these isotherms often fail to describe experimental data adequately. Freundlich (1926) found that adsorption equilibrium data were often better described by the relationship:

$$q_M = KC_M^{\frac{1}{n}} \qquad (2\text{-}58)$$

where K and n are empirical constants dependent on the nature of solid and adsorbate, and on temperature. The values of K and n need to be found by means of thermodynamic experiments. The experimental results are plotted firstly. A least square method was then used to produced a regression equation. The coefficient and power of the regression equation are the K and n values.

However, data for heavy metal adsorption onto volcanic ash soil is not available, but Yuan and Lavkulich (1997) studied the sorption behaviour of copper, zinc, and cadmium to other soils and found that adsorption of heavy metals fitted the Freundlich equation. Therefore, it is reasonable to believe that the Freundlich isotherm model can be used as an equilibrium description of the adsorption of copper to volcanic ash soil, but this assumption should be verified by an experiment.

2.4. Conclusion

Soil contaminated by heavy metal ions has become a global problem. Besides legislation to restrict further input of heavy metals to the soils, remediation is also required. The most common engineering means of remediation is leaching. Volcanic ash soil is common in New Zealand. No model was found for predicting the process of leaching heavy metals from volcanic ash soil in the literature. Developing a model to predict the process of leaching heavy metals from volcanic ash soil is important for New Zealand. There have been many studies published in this field, some of which relate to the development of a mathematical model. For example, there are mainly two different process models for the overall process of leaching, progressive conversion model (PCM) and shrinking unleached core model (SUCM). Because the latter approximates the real fluid-particle process more closely than does the former, shrinking unleached core model (SUCM) was used in the study. For internal diffusion of heavy metal ions within volcanic soil aggreagtes, there are also two different models, such as pore diffusion model and surface diffusion model. Only pore diffusion model was used in the study because no data could be collected for the surface diffusion coefficient.

Using water or an organic reagent to leach heavy metal from volcanic ash soil is a heterogeneous solubilization process. In the process, mass transfer and surface solubilization will occur simultaneously. Since volcanic ash soil is a highly and porous medium, more solubilization and mass transfer will occur in the interior than at the exterior of soil aggregates. Therefore, the influence of pores in volcanic ash soil on surface solubilization and diffusion in pores is important. The process is complex. Simplification or idealisation of the process is necessary to develop a model. However, this leads to a dilemma in model development. Simple modelling will result in a sacrifice of prediction accuracy; conversely, raising the prediction accuracy will lead to very complex modelling. Consequently, selecting and developing proper modelling to describe or simulate the process of leaching heavy metals from volcanic soil is difficult.

Development of a model predicting the leaching of heavy metal from contaminated

soil requires knowledge of the physical properties of the soil. However, some properties have not been studied and published. For example, no data on the liquid surface diffusion coefficient of electrolytes in soil was found. Many important physical parameters for volcanic ash soil can not be obtained from the literature. These physical parameters include porosity, tortuosity, size distribution and density of the aggregates of volcanic ash soils. Using other parameters to replace them may lead to lower accuracy of the model, but the decrease of accuracy may be tolerated. For instance, using bulk density (ρ_b) replaces aggregate density (ρ_a). However, some simplifications lack physical justification, but must be done, such as omitting surface diffusion because of no suitable surface diffusion coefficient.

CHAPTER 3

MATERIALS AND METHODS

3.1 Background

Among the five kinds of volcanic ash soils, Allophane is the most common volcanic ash soil in New Zealand. Therefore, it was chosen as experimental material in this study. The important physical properties about Allophane are listed in the following table (New Zealand Soil Bureau, 1968).

Table 3-1 Soil characteristics

Moisture (% w/w)	10.3
Dry bulk density (kg/m^3)	740
Total porosity (%)	68.0
Particle density((kg/m^3)	2610

From New Zealand Soil Bureau (1968)

In general, common heavy metals which appeared in contaminated soil are Copper, Zinc, Cadmium, Chromium, Manganese, Nickel, Lead. Copper was selected for the present study because it is easy to measure by atomic absorption spectrophotometer at different wavelengths. Each wavelength has an optimum work range. For copper, there are six different wavelengths for selection, so the range of copper ion concentration directly measured by atomic absorption spectrophotometer is very wide, about from 1ppm to 1700 ppm. The adsorbate selected was copper sulfate ($CuSO_4$) because it is cheap and easy to obtain. Only the deionized water was used in the study.

3.2 Collection and preparation of volcanic soil sample

Volcanic ash soil was collected from a site close to the Whareroa Road, opposite Kiwi Dairy Factory, New Zealand, in August 1999. The grass sod that covered the top

layer of soil was removed initially. The top layer of soil is also volcanic ash soil, but it is black and has different physical properties. This layer of soil was scraped during collection because it may contain more organic matter and heavy metals due to irrigation, fertilizer application and action of animal and plant. Under the top layer of soil, the color of this volcanic soil is brown, and it is this soil that was collected for investigation. The depth for collection of volcanic soil samples is about 33 ~ 41 cm. This layer of volcanic soil is considered to be rich in Allophane and undisturbed (New Zealand Soil Bureau, 1968).

The volcanic soil sample was first air dried. Then, the dried soil sample was sieved through an 850 μm screen to remove stones and large plant roots. Capillary plant roots ware removed by an electric fan blowing over the dried soil. Finally, British Standard sieves were used to obtain three different ranges of soil aggregate sizes, 600 ~ 800 μm, 500 ~ 600 μm and 425 ~ 500 μm. The average aggregate size of each range was determined from a plot of $1/d_p$ *versus* cumulative mass fraction, 700 μm, 550 μm and 460 μm. Before use, all soil samples were dried further at 38 °C until a constant weigh was achieved.

The copper content in the soil samples was negligible, and errors from this neglect are insignificant.

3.3 Analysis

All samples for copper sulfate from the bulk liquid were measured by using an atomic absorption spectrophotometer (GBC 933 AA, GBC Scientific Equipment Pty. Ltd.). The wavelength of the copper lamp in atomic absorption spectrophotometer was set at 324.7 nm generally. Under this wavelength, the sensitivity of the atomic absorption spectrophotometer for copper sulfate is the smallest, only about 0.025 mg/l. The optimum measurement range of concentration for copper sulfate was 1 ppm to 5 ppm, and samples were diluted with deionized water as needed. To minimise dilution error the wavelength may be changed if lighter concentrations are measured.

The atomic absorption spectrophotometer was warmed up for more than half an hour before use. In order to detect the systematic error from atomic absorption spectrophotometer, a sample of known concentration was measured in triplicate under the same condition. The relative errors from atomic absorption spectrophotometer must not be greater than 3%, otherwise it may not be useful checking a computer model with these experimental data. For unknown samples, the relative deviation must not be higher than 3%. If that occurred, the concentration of the sample would be remeasured until the relative deviation did not exceed more than 3%.

A set of standard solutions of copper sulfate (from 1 ppm to 5 ppm) was prepared in advance to determine a linear Calibration curve.

3.4 Experimental procedures

All preliminary, thermodynamic, kinetic and stirred vessel experiments were carried out at the same environmental conditions. In order to avoid the concentration change due to the volatilization of moisture content, all experimental containers were sealed. Each experiment was carried out in triplicate for three different aggregate sizes of volcanic soil samples, respectively.

In addition, because the aggregates of volcanic soil are not strong, prolonged and/or vigorous agitation of the mixture of soil sample and solution will lead to many aggregates being broken. Thus, the average diameter of soil aggregates might be changed significantly during the experiment if the experimental time is long.

3.4.1 Preliminary experiments

Preliminary experiments were carried out to find the equilibrium time for adsorption and desorption. In order to determine the time required to achieve equilibrium for adsorption, 0.5 grams and 2.5 grams of each size soil sample were contacted with 100 ml known concentration solution of copper sulfate in a 250 ml flask, respectively. Then, the

flasks containing mixtures of solution and soil sample were placed in a thermostatic orbital incubator (Gallenkamp) for shaking. The operating conditions of this shaker were set up at 25 °C and 140 rpm. At given time intervals, flasks were taken out from the shaker and settled for a few minutes. The supernatant was filtered by using glass fiber filter paper with a pore size of 1.2 μm and was analyzed by an atomic absorption spectrophotometer to determine the concentration of copper sulfate. After about eight hours, the rate of concentration change for copper sulfate solution in the bulk liquid with time was not significant when the experiment was terminated.

The equilibrium time for desorption was determined by the same procedure using soil samples with adsorbed copper sulfate in place of fresh soil samples. The soil samples with adsorbed copper sulfate were prepared in advance by contacting fresh volcanic soil with a solution of copper sulfate till adsorption equilibrium was attained. Once adsorption equilibrium was achieved, the volcanic soil with adsorbed copper sulfate was separated from the mixture by using a vacuum filter. Finally, the dewatered soil sample was dried in a thermostatic dryer at 38 °C before use. The desorption equilibrium time was found to be about four hours.

3.4.2 Thermodynamic experiments

The aim of the thermodynamic experiments was to determine which equilibrium relationship exists and to determine the corresponding parameters for use in the study. The adsorption of heavy metals onto non-volcanic soil was described by Freundlich isotherm (Yuan and Lavkulich, 1997), but no literature on Freundlich equilibrium relationship for adsorption or desorption of heavy metals onto volcanic soil was found.

The experimental procedure for thermodynamic experiments was the same as that for the preliminary experiments. Ten flasks contained different weights of soil samples (from 0.25 grams to 2.5 grams) and 100 ml of a known concentration solution of copper sulfate. In order to ensure that adsorption equilibrium was achieved, all flasks were placed in the shaker for at least 24 hours. The difference between the initial and final concentration of

copper sulfate in the bulk liquid was taken to be the result of adsorption. Experiments were duplicated for all volcanic soil samples of the three different sizes.

The procedures for investigating desorption equilibrium was the same as for adsorption equilibrium. However, the soil samples used were the dried soil with adsorbed copper sulfate instead of the fresh volcanic soil sample, prepared as described in preliminary experiments.

3.4.3 Kinetic experiments

The kinetic experiments were carried out to find the rate of change in the concentration of copper sulfate in the bulk liquid with time and to compare this with the computer model predictions. In these adsorption kinetic experiments, a solution of known concentration of copper sulfate was contacted with 2.5 grams of fresh volcanic soil sample and continuously shaken in a thermostatic shaker. The flasks were taken out of the thermostatic shaker at different time interval and the concentration of copper sulfate in the bulk liquid in this flask was measured by atomic absorption spectrophotometer. The experiment continued until equilibrium was reached (about 24 hours).

Desorption kinetic experiments were carried out with the same method as adsorption kinetic experiment using dried volcanic soil with adsorbed copper sulfate. The experiment was conducted over 24 hours.

3.4.4 Stirred vessel experiments

Stirred vessel experiments were carried out to simulate the real leaching process and to validate the kinetic model. The cycle for the stirred vessel experiments was the same as for the above kinetic experiments.

The "contaminated" soil and water are put into the stirred vessel simultaneously, and an impeller is used to stir the mixture of liquid and solid. The rotation rate of the impeller

was kept constant. The separation of liquid and solid was carried out as soon as the bulk liquid concentration of heavy metal remained unchanged. The cycle for the batch stirred process includes three steps: feeding, stirring and discharging. Figure 3-1 shows the sketch of the process.

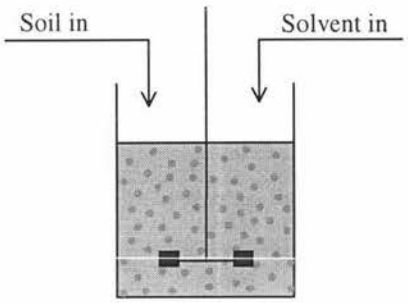

Figure 3-1 Sketch of stirred process

A stirred vessel that had a volume of more than eight liters with four baffles was used. The internal diameter of this vessel was 0.19 m. Five liters of deionized water and six grams of dried volcanic soil with adsorbed copper sulfate were placed in the stirred vessel. The mixture of soil and solution was agitated by a four-blade disk turbine with external diameter of 0.092m. The installation depth of impeller in the vessel was about 0.05m from the bottom of the vessel, and the stirring speed was about 450 rpm. The copper sulfate adsorbed on the surface of volcanic soil was released gradually to the bulk liquid under continuous stirring. The concentration of copper sulfate was measured by atomic absorption spectrophotometer at the time intervals of 0.25, 0.50, 1.00, 2.00, 3.00, 4.00, 5.50, 7.00, 8.50, 10.00, and 24.00 hour.

The sample size was less than 8 ml from 5 liters volume. The total volume of liquid in the stirred vessel was not changed significantly and therefore the distribution of the velocity field in the vessel did not change significantly either.

3.5 Mathematical methods

The mathematical models used in this project include a second order partial differential equation and a first order original differential equation. Unfortunately, the two differential equations have no analytical solutions because the coefficients in these differential equations are not constant, and are complex functions of concentration. Therefore, these mathematical models were solved using numerical analysis. In order to

solve these equations by numerical analysis, all differential equations should be translated to finite difference equations. This is the method of finite difference approximation. The principle of finite difference approximation is replacing an infinite differential with a finite difference plus error term. By means of appropriately selecting the step size value for the independent variable, the errors can be within the acceptable level. Besides the method, there are some other ways, such as finite elements.

There are three finite difference approximations:

- The forward difference approximation

$$\frac{\partial f(x,y)}{\partial x} = \frac{f(x+\Delta x,y)-f(x,y)}{\Delta x} + e(\Delta x) \qquad (3\text{-}1)$$

- The backward difference approximation

$$\frac{\partial f(x,y)}{\partial x} = \frac{f(x,y)-f(x-\Delta x,y)}{\Delta x} + e(\Delta x) \qquad (3\text{-}2)$$

- The central difference approximation

$$\frac{\partial f(x,y)}{\partial x} = \frac{f(x+\Delta x,y)-f(x-\Delta x,y)}{2\Delta x} + e((\Delta x)^2) \qquad (3\text{-}3)$$

where $e(\Delta x)$ and $e((\Delta x)^2)$ are the error terms. For parabolic partial differential equations, different combination of these three finite difference approximations results in different difference methods. Using forward difference approximation will give one of the simplest difference techniques. The technique is best known as the explicit difference method because each new value of the dependent variable can be immediately calculated from quantities that are already known. It is simple and economical to calculate, and is similar in spirit to partial differential equation. However, there is a restrictive condition for the method, which means that the method is conditionally stable. If only some conditions are met may the numerical solution of the differential equation be stable. The Crank-Nicolson method from the average of forward and backward differential approximations

is implicit. It is unconditionally stable but complex. The method needs to use matrix calculus, which will lead to a complicated computer program.

In order to simulate and predict the process of leaching heavy metals from volcanic ash soil by water using a computer, a computer program was necessary. The program was written in PASCAL in the present study.

CHAPTER 4

THERMODYNAMIC AND KINETIC MODEL

4.1 Introduction

Thermodynamic and kinetic models of each chemical or physical process must be essential bases for developing a computer model. A thermodynamic model is an equilibrium relationship, and it indicates the limit of a process. The kinetic model is based on diffusion including an internal diffusion model (pore and surface diffusion model) (Noll et al., 1992) and an external diffusion model (film transport diffusion model).

Better understanding the mechanism of adsorption and desorption of heavy metals in volcanic soil is important for simulating the process and selection of clean-up methods. Simplifying and idealizing the process are necessary for establishing a model. Thus, an accurate judgment is required to determine which parameters of the process are important or not for developing a computer model.

The explicit method was used to translate the partial differential equation of second into a set of finite difference equations. The advantage of the numerical algorithm is the ease of programming. However, the method limits the selection of a time step that is dependent on space step. In order to obtain a higher accuracy, the space step is not large. Therefore, the time step needs to be small enough, so the time running the computer program may be very long.

The heat effect of adsorption and desorption of heavy metal ions in volcanic ash soil is very small, and there is no obvious temperature change during adsorption or

desorption. In addition, the process is reversible. Therefore, the processes can be treated as physical adsorption and desorption without inclusion of temperature effects.

4.2 Thermodynamic model

A process will be in a state of dynamic equilibrium if its limit is attained. Isotherm equations were used to model the equilibrium state of adsorption and desorption. There have been several thermodynamic models published by some researcher. These models include a linear model (Henry' Law), the Langmuir model, BET model, Gibbs model, and the Freundlich model (Slejko, 1985). Among these thermodynamic models, the Freundlich model may be the most suitable equilibrium equation describing adsorption-desorption of heavy metal ions in volcanic soil because the conditions of the heavy metal-volcanic soil system is the closest to the basic assumptions of the model. For example, the system is constituted by a liquid phase and a solid phase, and the attraction between heavy metal ions and volcanic soil or between heavy metal ions is in the field of van der Waals forces, and there is no chemical reaction involved.

In addition, the adsorption of heavy metal ions on the surface of soil is a typical favorable adsorption, which is characterized by the occurrence of adsorption at low concentration in the bulk liquid. Because the heavy metals ions adsorbed on the surface of volcanic soil are involved in neither association nor dissociation, the adsorption equilibrium can be expressed by the Freundlich model.

$$q_M = KC_M^{\frac{1}{n}} \qquad (4\text{-}1)$$

In general, a large number of experimental results in the field of van der Waals adsorption can be expressed by means of the Freundlich equation in the middle concentration range (Noll et al., 1992). According to the Freundlich equation, the amount adsorbed increases infinitely with increasing concentration. This equation is, therefore, unsatisfactory for high coverage. At low concentration, this equation does not reduce to a linear isotherm. These are typical characteristics of non-monolayer physical adsorption.

The empirical constants in the Freundlich equation are dependent on the nature of soil and adsorbate, and temperature. They can be obtained from experimental data by means of regression analysis.

4.3 Kinetic models

Kinetics is used to describe the rate of a process, which is important for efficient and economical production in industry. Therefore, it is necessary to build an appropriate kinetic model in simulating an actual process. In general, kinetic models can be established by means of material or energy balance for the process studied.

For an adsorption or desorption process, heterogeneous and homogeneous mass transfer are involved simultaneously because there are at least two phases in the system. The diffusion mechanisms are different for internal diffusion and external diffusion, so the kinetic models for a single particle and for a stirred vessel need to be developed respectively.

4.3.1 Diffusion model for a single aggregate

Volcanic soil aggregates are heterogeneous systems formed by a porous solid phase and a fluid phase filling the void fraction of the solid, so the mass transfer in volcanic soil aggregates is heterogeneous mass transfer. On the internal pore surface, an adsorbate in the solid phase may move along the surface when it attains sufficient activation energy and when an adjacent adsorption site is available. Although the mobility of the adsorbed phase will generally be smaller than that in the solution, the concentration is much higher, so a significant contribution to flux is possible.

Only if a substance accumulates generously onto the surface of a solid can the surface diffusion be considered important, so it does not exist always. For example, there is not any surface diffusion in some non-adsorption surface processes, such as ion exchange and fluid-solid chemical reactions. However, the pore diffusion always occurs along with

all surface processes because it is independent of the surface accumulation. Therefore, the internal diffusion for the adsorption and desorption processes of heavy metal ions in a single volcanic soil aggregate should be expressed by surface diffusion and pore diffusion simultaneously. The transport mechanisms in a soil aggregate are shown in Figure 2-5.

Because volcanic soil aggregates are very small and the soil samples were screened by a set of sieves before using them, the aggregates can be assumed to be spherical and of uniform size. Figure 4-1 shows a sketch of mass transport in a spherical soil aggregate. The internal diffusion model for volcanic soil aggregates can be derived by making a material balance on heavy metal ions for a small element of the intra-particle distance.

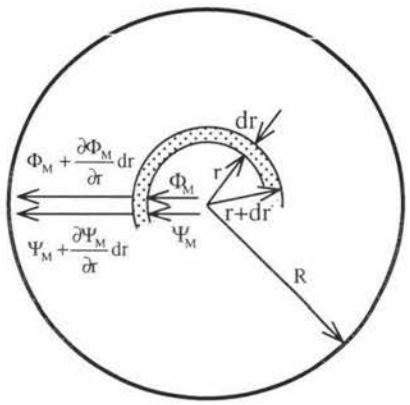

Figure 4-1 Sketch of mass transport in a aggregate

If this combined parallel resistance within the adsorbent particle is considered, a material balance on heavy metal ions for the small element results in the following partial differential equations is:

Accumulating rate of H. M. ions in pore at the element	+	Accumulating rate of H. M. ions on surface of liquid at the element	=	The pore diffusion rate of H. M. ions into the element	-	The pore diffusion rate of H. M. ions out of the element	+	The surface diffusion rate of H. M. ions into the element	-	The surface diffusion rate of H. M. ions out of the element

Translated the word balance equation to mathematics equation:

$$\varepsilon V\frac{\partial C_M}{\partial t}+\rho_{as}V\frac{\partial q_M}{\partial t}=\varepsilon A_r\cdot\Phi_M-\varepsilon A_{r+dr}\cdot(\Phi_M+\frac{\partial \Phi_M}{\partial r}dr)+\rho_{as}A_r\cdot\Psi_M-\rho_{as}A_{r+dr}\cdot(\Psi_M+\frac{\partial \Psi_M}{\partial r}dr) \quad (4\text{-}2)$$

A_r and A_{r+dr} are diffusion areas at r and r+dr, respectively. They can be calculated by following two formulae:

$$A_r = 4\pi \cdot r^2 \tag{4-3}$$

$$A_{r+dr} = 4\pi \cdot (r+dr)^2 \tag{4-4}$$

Substitute equations (4-3) and (4-4) into equation (4-2) and neglect second or higher infinitesimal, equation (4-2) changed to:

$$\varepsilon V\frac{\partial C_M}{\partial t}+\rho_{as}V\frac{\partial q_M}{\partial t}=-4\pi\varepsilon\cdot(r^2\frac{\partial \Phi_M}{\partial r}+2r\cdot\Phi_M)dr-4\pi\rho_{as}\cdot(r^2\frac{\partial \Psi_M}{\partial r}+2r\cdot\Psi_M)dr \tag{4-5}$$

Φ_M and Ψ_M are the pore diffusion flux and surface diffusion flux, respectively. They can be described by Fick's first law:

$$\Phi_M = -D_{eM}\frac{\partial C_M}{\partial r} \tag{4-6}$$

$$\Psi_M = -D_{sM}\frac{\partial q_M}{\partial r} \tag{4-7}$$

Equation (4-5) can also be rewritten by using the following method:

$$\because x^2\frac{\partial y}{\partial x}+2xy=\frac{\partial}{\partial x}(x^2y) \tag{4-8}$$

$$\therefore \varepsilon V\frac{\partial C_M}{\partial t}+\rho_{as}V\frac{\partial q_M}{\partial t}=-4\pi\varepsilon\cdot\frac{\partial}{\partial r}(r^2\cdot\Phi_M)dr-4\pi\rho_{as}\cdot\frac{\partial}{\partial r}(r^2\cdot\Psi_M)dr \tag{4-9}$$

V is the volume of the small element and is expressed by the following formula:

$$V=\frac{4}{3}\pi\cdot[(r+dr)^3-r^3] \tag{4-10}$$

Substitute equation (4-6) and equation (4-7) into equation (4-9) and divide it by V, and

then neglected second or higher infinitesimal, the internal diffusion model can be obtained:

$$\varepsilon\frac{\partial C_M}{\partial t}+\rho\frac{\partial q_M}{\partial t}=\frac{\varepsilon}{r^2}\frac{\partial}{\partial r}(r^2 D_{eM}\frac{\partial C_M}{\partial r})+\frac{\rho}{r^2}\frac{\partial}{\partial r}(r^2 D_{sM}\frac{\partial q_M}{\partial r}) \qquad (4\text{-}11)$$

The internal diffusion model is a partial differential equation of the second order. The first term on the right side of the above equation represents the pore diffusion, and the second term expresses the surface diffusion. The equation can describe the internal diffusion of spherical particle either for adsorption or for desorption process.

In order to solve the partial differential equation (4-11), two boundary conditions and one initial condition are required. On the exterior surface of the soil aggregate, an assumption of no mass accumulating on the exterior surface is done, so the first boundary condition can be derived by mass balance:

Mass of solute from interior to surface of soil aggregate by internal diffusion	=	Mass of solute away the surface of soil aggregate to liquid phase by external diffusion

In mathematical terms that becomes:

$$A_R(\varepsilon\cdot\Phi_M+\rho_{as}\cdot\Psi_M)=A_R\cdot k_{lM}(C_{sM}-C_{lM}) \qquad (4\text{-}12)$$

Simplifying equation (4-12) the following equation can be obtained:

$$\varepsilon D_{eM}\frac{\partial C_M}{\partial r}+\rho_{as}D_{sM}\frac{\partial q_M}{\partial r}=\varepsilon\cdot k_{lM}(C_{lM}-C_{sM}) \qquad (4\text{-}13)$$

At the center of the soil aggregate the boundary is symmetric, so the second boundary condition is expressed as:

$$\left.\begin{aligned}\frac{\partial C_M}{\partial r}&=0\\ \frac{\partial q_M}{\partial r}&=0\end{aligned}\right\} \qquad \text{at } r=0 \text{ for } t\geq 0 \qquad (4\text{-}14)$$

The initial condition assumes that the concentration of copper sulfate in the bulk liquid is a constant initially:

$$\left.\begin{aligned}C_M&=C_{Mi}\\ q_M&=q_{Mi}\end{aligned}\right\} \qquad 0\leq r\leq R \text{ for } t=0 \qquad (4\text{-}15)$$

If the local equilibrium relationship conforms to the Freundlich isotherm and is achieved quickly, equation (4-11) can be rewritten.

$$\because \frac{\partial q_M}{\partial r}=\frac{\rho_{as}K}{n}C_M^{\frac{1}{n}-1}\cdot\frac{\partial C_M}{\partial r} \qquad (4\text{-}16)$$

$$\therefore(\varepsilon+\frac{\rho_{as}K}{n}C_M^{\frac{1}{n}-1})\frac{\partial C_M}{\partial r}=\frac{\varepsilon}{r^2}\frac{\partial}{\partial r}(r^2D_{eM}\frac{\partial C_M}{\partial r})+\frac{\rho_{as}K}{r^2n}\frac{\partial}{\partial r}(r^2D_{sM}C_M^{\frac{1}{n}-1}\frac{\partial C_M}{\partial r}) \qquad (4\text{-}17)$$

Equation (4-17) can be rewritten to:

$$(\varepsilon+\frac{\rho_{as}K}{n}C_M^{\frac{1}{n}-1})\frac{\partial C_M}{\partial r}=\frac{1}{r^2}\frac{\partial}{\partial r}[r^2(\varepsilon D_{eM}+\frac{\rho_{as}K}{n}D_{sM}C_M^{\frac{1}{n}-1})\frac{\partial C_M}{\partial r}] \qquad (4\text{-}18)$$

Correspondingly, the boundary and initial conditions change to:

$$\frac{\partial C_M}{\partial r}=0 \qquad \text{at } r=0 \text{ for } t\geq 0 \qquad (4\text{-}19)$$

$$(\varepsilon D_{eM}+\frac{\rho_{as}K}{n}D_{sM}C_M^{\frac{1}{n}-1})\frac{\partial C_M}{\partial r}=\varepsilon k_{lM}(C_{lM}-C_{sM}) \quad \text{at } r=R \text{ for } t\geq 0 \qquad (4\text{-}20)$$

$$\left.\begin{aligned}C_M&=C_{Mi}\\ q_M&=KC_{Mi}^{\frac{1}{n}}\end{aligned}\right\} \qquad 0\leq r\leq R \text{ for } t=0 \qquad (4\text{-}21)$$

If the surface diffusion coefficient, D_{sM}, can be explicitly expressed by a formula or a table, or implicitly expressed by a solvable equation, the equations (4-18), (4-19), (4-20) and (4-21) can be solved by using numerical analysis such as the fourth order Runge-Kutta technique. The equation (4-18) should be the most accurate to describe the internal diffusion of heavy metal ions in volcanic soil aggregates. However, the surface diffusion coefficient is difficult to obtain.

As the internal diffusion is the pore process control, which means that the surface diffusion coefficient, D_{sM}, is much less than the pore diffusion coefficient, D_{eM}, the surface diffusion can be ignored. Therefore, the equation (4-2) can be reduced to:

$$\varepsilon\frac{\partial C_M}{\partial t}+\rho_{as}\frac{\partial q_M}{\partial t}=\varepsilon\frac{\partial}{\partial r}(D_{eM}\frac{\partial C_M}{\partial r})+\varepsilon\frac{2D_{eM}}{r}\frac{\partial C_M}{\partial r} \qquad (4\text{-}22)$$

The boundary and initial conditions of equation (4-22) are:

$$\frac{\partial C_M}{\partial r}=0 \qquad \text{at } r=0 \text{ for } t\geq 0 \qquad (4\text{-}23)$$

$$D_{eM}\frac{\partial C_M}{\partial r}=k_{lM}(C_{lM}-C_{sM}) \qquad \text{at } r=R \text{ for } t\geq 0 \qquad (4\text{-}24)$$

$$\left.\begin{aligned} C_M &= C_{Mi} \\ q_M &= q_{Mi} \end{aligned}\right\} \qquad 0\leq r\leq R \text{ for } t=0 \qquad (4\text{-}25)$$

As the local equilibrium is achieved quickly and can be expressed as a Freundlich isotherm, equation (4-22) can be rewritten to:

$$(\varepsilon+\frac{\rho_{as}K}{n}C_M^{\frac{1}{n}-1})\frac{\partial C_M}{\partial t}=\varepsilon\frac{\partial}{\partial r}(D_{eM}\frac{\partial C_M}{\partial r})+\varepsilon\frac{2D_{eM}}{r}\frac{\partial C_M}{\partial r} \qquad (4\text{-}26)$$

The boundary and initial conditions of equation (4-26) are:

$$\frac{\partial C_M}{\partial r} = 0 \qquad \text{at } r = 0 \text{ for } t \geq 0 \tag{4-27}$$

$$D_{eM} \frac{\partial C_M}{\partial r} = k_{lM}(C_{lM} - C_{sM}) \qquad \text{at } r = R \text{ for } t \geq 0 \tag{4-28}$$

$$C_M = C_{Mi} \qquad 0 \leq r \leq R \text{ for } t = 0 \tag{4-29}$$

In the study, the kinetic model used in the computer program is equation (4-26) and its boundary and initial conditions equations (4-27), (4-28) and (4-29).

4.3.2 Diffusion model for stirred vessel

In a stirred vessel, the bulk liquid is the continuous phase and the volcanic soil aggregates are the dispersed phase. Therefore, the mass transfer from the external surface of volcanic soil aggregates to the main body of liquid is homogeneous mass transfer. The resistance of mass transfer concentrates mainly in the liquid film around the volcanic soil aggregates. In order to obtain an equation describing the change of heavy metal ion concentration in the bulk liquid in a stirred vessel with time for batch operation process, a material balance on heavy metal ions for the vessel is:

Accumulating rate of H. M. ions in bulk liquid in the vessel	=	Releasing rate of H. M. ions from soil aggregates to bulk liquid

Translating the word balance equation into mathematical equation:

$$V_l \frac{\partial C_{lM}}{\partial t} = n_a \cdot \varepsilon A_R k_{lM}(C_{sM} - C_{lM}) \tag{4-30}$$

where V_l is the volume of the liquid in the stirred vessel (m^3); A_R is the surface area of a single volcanic soil aggregate (m^2) and it can be calculated by the following equation:

$$A_R = 4\pi R^2 \tag{4-31}$$

n_a is the total number of soil aggregates in the vessel and it is expressed by the following equation:

$$n_a = \frac{W_t}{V_a \rho} \tag{4-32}$$

where W_t is the total weight of the dry volcanic soil in the vessel (kg); V_a is the volume of a single soil aggregate (m^3).

This is an ordinary differential equation of the first order for time, so only the initial condition is needed to solve this ordinary differential equation. The initial condition for this ordinary differential equation is:

$$C_{lM} = C_{lMi} \qquad R \leq r \text{ for } t = 0 \tag{4-33}$$

Because k_{lM} is not a constant over time, there is not an analytic solution for this ordinary differential equation. Therefore, equations (4-30) and (4-33) have to be solved by numerical methods.

4.4 Algorithm

To solve the above partial differential equation and ordinary differential equation with a computer program, these equations can be transferred to finite difference equations. There are two different ways for doing this, implicit and explicit methods. The explicit method was used in this study because it is easier to write and understand a computer program than the implicit method.

4.4.1 Finite difference equation

The diffusion coefficient of copper sulfate in water is not a constant. It depends on the concentration of copper sulfate in water. However, the change in diffusion coefficient with concentration is not significant, changes from 7.34×10^{-10} to 8.57×10^{-10} m^2/s as the concentration of copper sulfate in bulk liquid changes from 100 ppm to 1 ppm. The use

of the explicit method is accurate enough as long as an appropriate selection of the steps for space and time for the finite difference equations has been done.

4.4.1.1 For volcanic soil aggregates

Because the concentration of copper sulfate in volcanic soil aggregates is not only a function of time but also of space, the equation describing internal diffusion of heavy metal ions in soil aggregates must be a partial differential equation with two independent variables, time and radius. The radius of volcanic soil aggregate was divided into J nodes. Thus, the step for space, Δr, can be expressed:

$$\Delta r = \frac{R}{J} \tag{4-34}$$

The larger the number of nodes, the smaller the step for space with a fixed value of volcanic soil aggregate size. In each node, the concentration of copper sulfate was assumed to be constant. Therefore, the infinite differential equation can be transferred into finite difference equation.

The step of time, Δt, is made small enough, so that the numerical solution of the partial differential equation is reliable. However, an overly small time step will lead to a very long run time, sometimes leading to a runtime error when running the computer program.

In order to solve the partial differential equation by means of numerical analysis, it should be translated to a finite difference equation. In general, after dividing into nodes and marking them, making a material balance for each node results in a series of finite difference equations. Surface diffusion flux was ignored, and only pore diffusion flux was considered. The following are the details for translation:

At the center node, (j = 0), because of the symmetry, no heavy metal ions were transferred into the node and there is only transport of heavy metal ions leaving this note

by diffusion, and only mass transport in one direction needs to be considered. Therefore, this is the simplest case in all notes. The details for mass transport at center node are shown in Figure 4-2. Making a mass balance for this node results in the following equation:

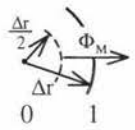

Figure 4-2 Sketch of mass transport at center node

$$V_{\frac{1}{2}} \cdot [\varepsilon + \frac{\rho_{as} K}{n} (C_{M0}{}^{i})^{\frac{1}{n}-1}] \cdot \frac{C_{M0}{}^{i+1} - C_{M0}{}^{i}}{\Delta t} = 0 - \varepsilon A_{\frac{1}{2}} \Phi_{M\frac{1}{2}} \tag{4-35}$$

where $V_{\frac{1}{2}}$ and $A_{\frac{1}{2}}$ are volume and area at $\frac{\Delta r}{2}$.

$$V_{\frac{1}{2}} = \frac{4\pi}{3} \cdot (\frac{\Delta r}{2})^3 \tag{4-36}$$

$$A_{\frac{1}{2}} = 4\pi \cdot (\frac{\Delta r}{2})^2 \tag{4-37}$$

$\Phi_{M\frac{1}{2}}$ is the pore diffusion flux at $\frac{\Delta r}{2}$.

$$\Phi_{M\frac{1}{2}} = -D_{eM\frac{1}{2}} \frac{C_{M1}{}^{i} - C_{M0}{}^{i}}{\Delta r} \tag{4-38}$$

Substitute equation (4-36), (4-37), and (4-38) into equation (4-35), then simplify, and then the equation changes to:

$$[\varepsilon + \frac{\rho_{as} K}{n} (C_{M0}{}^{i})^{\frac{1}{n}-1}] \cdot \frac{C_{M0}{}^{i+1} - C_{M0}{}^{i}}{\Delta t} = \frac{6\varepsilon}{\Delta r^2} D_{eM\frac{1}{2}} (C_{M1}{}^{i} - C_{M0}{}^{i}) \tag{4-39}$$

Rearrange the above equation as:

$$C_{M0}{}^{i+1} = C_{M0}{}^{i} + \frac{6\frac{\varepsilon \cdot \Delta t}{\Delta r^2} D_{eM\frac{1}{2}} (C_{M1}{}^{i} - C_{M0}{}^{i})}{\varepsilon + \frac{\rho_{as} K}{n} (C_{M0}{}^{i})^{\frac{1}{n}-1}} \tag{4-40}$$

For internal nodes, j = 1 to J-1, the mass transport for these nodes are shown in Figure 4-3. Using the same procedure as for the center node, the finite difference equation for internal nodes can be derived. However, there is not only mass transport out but also mass transport in for these nodes. Therefore, using mass balance can derive the finite difference equation for these nodes:

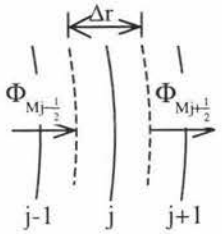

Figure 4-3 Mass transport at node j

$$V_j \cdot [\varepsilon + \frac{\rho_{as} K}{n} (C_{Mj}{}^{i})^{\frac{1}{n}-1}] \cdot \frac{C_{Mj}{}^{i+1} - C_{Mj}{}^{i}}{\Delta t} = \varepsilon A_{j-\frac{1}{2}} \Phi_{Mj-\frac{1}{2}} - \varepsilon A_{j+\frac{1}{2}} \Phi_{Mj+\frac{1}{2}} \quad (4\text{-}41)$$

$$V_j = \frac{4\pi}{3} \cdot (\Delta r)^3 \cdot [(j+\frac{1}{2})^3 - (j-\frac{1}{2})^3] \quad (4\text{-}42)$$

$$A_{j-\frac{1}{2}} = 4\pi \cdot (\Delta r)^2 \cdot (j-\frac{1}{2})^2 \quad (4\text{-}43)$$

$$A_{j+\frac{1}{2}} = 4\pi \cdot (\Delta r)^2 \cdot (j+\frac{1}{2})^2 \quad (4\text{-}44)$$

Substitute equation (4-42), (4-43), and (4-44) into equation (4-41), and then simplify that, the equation changes to:

$$[\varepsilon + \frac{\rho_{as} K}{n} (C_{Mj}{}^{i})^{\frac{1}{n}-1}] \frac{C_{Mj}{}^{i+1} - C_{Mj}{}^{i}}{\Delta t} = \frac{\varepsilon}{\Delta r^2} \frac{(j-\frac{1}{2})^2}{(j^2+\frac{1}{12})} D_{eMj-\frac{1}{2}} (C_{Mj-1}{}^{i} - C_{Mj}{}^{i}) - \frac{\varepsilon}{\Delta r^2} \frac{(j+\frac{1}{2})^2}{(j^2+\frac{1}{12})} D_{eMj+\frac{1}{2}} (C_{Mj}{}^{i} - C_{Mj+1}{}^{i}) \quad (4\text{-}45)$$

Rearrange the above equation to:

$$C_{Mj}{}^{i+1} = C_{Mj}{}^{i} + \frac{\frac{\varepsilon \cdot \Delta t}{\Delta r^2} [(j-\frac{1}{2})^2 \cdot D_{eMj-\frac{1}{2}} (C_{Mj-1}{}^{i} - C_{Mj}{}^{i}) - (j+\frac{1}{2})^2 \cdot D_{eMj+\frac{1}{2}} (C_{Mj}{}^{i} - C_{Mj+1}{}^{i})]}{[\varepsilon + \frac{\rho_{as} K}{n} (C_{Mj}{}^{i})^{\frac{1}{n}-1}] \cdot (j^2 + \frac{1}{12})} \quad (4\text{-}46)$$

For the surface node, j = J, although there is mass transport in and out, the mechanism

of mass transport out is different from internal diffusion, and it is an external diffusion. The external diffusion will be affected by the velocity of liquid in the stirred vessel. Figure 4-4 shows the details of mass transport at surface node. The finite difference equation can be derived by performing a mass balance for the node:

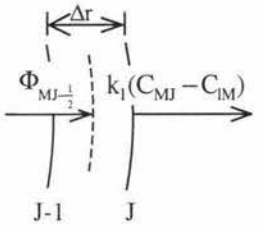

Figure 4-4 Mass transport at surface node

$$V_J \cdot [\varepsilon + \frac{\rho_{as} K}{n}(C_{MJ}{}^{i})^{\frac{1}{n}-1}]\frac{C_{MJ}{}^{i+1} - C_{MJ}{}^{i}}{\Delta t} = \varepsilon A_{J-\frac{1}{2}} \Phi_{MJ-\frac{1}{2}} - \varepsilon A_J \cdot k_{lM}(C_{MJ}{}^{i} - C_{lM}{}^{i}) \quad (4\text{-}47)$$

Divide equation (4-47) by V_J and simplify it, the following equation can be obtained:

$$[\varepsilon + \frac{\rho_{as} K}{n}(C_{MJ}{}^{i})^{\frac{1}{n}-1}]\frac{C_{MJ}{}^{i+1} - C_{MJ}{}^{i}}{\Delta t} = \frac{\varepsilon}{\Delta r^2}\frac{2(J-\frac{1}{2})^2}{[(J-\frac{1}{4})^2 + \frac{1}{48}]} D_{eMJ-\frac{1}{2}}(C_{MJ-1}{}^{i} - C_{MJ}{}^{i}) - \frac{2\varepsilon}{\Delta r^2}\frac{2J^2}{[(J-\frac{1}{4})^2 + \frac{1}{48})} k_{lM}(C_{MJ}{}^{i} - C_{lM}{}^{i}) \quad (4\text{-}48)$$

Rearrange equation (4-48) to:

$$C_{MJ}{}^{i+1} = C_{MJ}{}^{i} + \frac{\frac{2\varepsilon \cdot \Delta t}{\Delta r^2}[(J-\frac{1}{2})^2 \cdot D_{eMJ-\frac{1}{2}}(C_{MJ-1}{}^{i} - C_{MJ}{}^{i}) - J^2 \cdot \Delta r \cdot k_{Ml}(C_{MJ}{}^{i} - C_{lM}{}^{i})]}{[\varepsilon + \frac{\rho_{as} K}{n}(C_{MJ}{}^{i})^{\frac{1}{n}-1}] \cdot [(J-\frac{1}{4})^2 + \frac{1}{48}]} \quad (4\text{-}49)$$

4.4.1.2 For stirred vessel

The concentration of copper sulfate in the main body of the well mixed liquid is only a function of time, and independent of space, so no nodes are needed. Only one finite difference equation is given. Therefore, the finite difference equation can be derived immediately from equation (4-30):

$$C_{lM}{}^{i+1} = C_{lM}{}^{i} + \frac{\Delta t}{V_l} \cdot n_a \cdot \varepsilon \cdot 4\pi(\Delta r)^2 J^2 \cdot k_{lM}(C_{MJ}{}^{i} - C_{lM}{}^{i}) \quad (4\text{-}50)$$

The liquid mass transfer coefficient, k_l, is a function of the velocity of volcanic soil

aggregates in the stirring vessel. In order to calculate the velocity, the Reynolds' number needs to be known in advance. However, velocity is an essential prerequisite for calculation of the Reynolds' number. Therefore, a trial and error method needs to be used for the calculation of velocity.

4.4.2 Solution stability

One of the disadvantages of the explicit method is that there is a relationship between the steps of time and space. In other words, once the step of space, Δr, is selected, the step of time, Δt, can no longer be selected randomly, otherwise the numerical solution may be not stable and reliable. Only if the selection of the step of time meets some condition, the numerical solution may be stable and reliable.

According to the theorem of stable numerical solutions for partial differential equations, the essential condition that there is a stable numerical solution for the partial differential equation (4-26) is that the coefficient of $C_{Mj}^{\ i}$ for equation (4-46) must be greater than zero. Therefore, the relationship between the step of time and that of space is:

$$\Delta t < \frac{\Delta r^2 \cdot [\varepsilon + \frac{\rho_{as} K}{n} (C_{Mj}^{\ i})^{\frac{1}{n}-1}] \cdot (j^2 + \frac{1}{12})}{\varepsilon \cdot [(j-\frac{1}{2})^2 \cdot D_{eMj-\frac{1}{2}} + (j+\frac{1}{2})^2 \cdot D_{eMj+\frac{1}{2}}]} \qquad (4\text{-}51)$$

Because C_M and D_{eM} are not constants, they will change with time, which means that the selected Δt may not meet equation (4-51) in some situations. Therefore, selecting Δt should be done very careful to make it suitable over the whole concentration range.

In general, the step of time should be smaller than that of space. Therefore, if the step of space is smaller, then the computer running time may be very long. For the implicit method, the selection of the step of time is independent of that of space.

4.5 Summary

The adsorption and desorption equilibrium model used in this study is the Freundlich isotherm. The constants of Freundlich isotherm are only determined by experiments because Freundlich isotherm is an empirical formula.

Kinetic models can be derived from a material balance. There are two different kinetic models, internal diffusion model for a single soil aggregate and external mass transfer model for stirred vessel. For the former, this is a second order partial differential equation. The later is a first order original differential equation.

For the internal diffusion model, equation (4-11) is most ideal because restrictive conditions required are the least for this equation. The assumption of a spherical aggregate is only a requirement. However, the surface diffusion coefficient (D_{sM}) is difficult to obtain. It is necessary to neglect the surface diffusion, which results in a simpler partial differential equation without surface diffusion. This is equation (4-22). The conclusion of this project is unsuitable for any processes of non-pore diffusion control.

In order to simulate the process of leaching copper (II) from volcanic soil by a computer model, all differential equations should be translated to finite difference equations. In this study, forward time method was used. The advantages for the method include simple, easy to understand and use, and similar form with differential equations, so it is easy to debug during computer program. However, the method is conditionally stable. That means the numerical solution for these differential equations may be unstable and bigger errors may be made.

The computer model was composed by the equilibrium model, kinetic models, and some formulae to calculate parameters. Therefore, it can only be used to predict the leaching process of a single metal ion in a spherical aggregate without surface diffusion,

and local equilibrium in conformity with the Freundlich isotherm. The computer program was written in PASCAL.

CHAPTER 5

RESULTS AND DISCUSSION

5.1 Introduction

In this chapter, the data from the experiment and the computer model are compared and discussed. The results of preliminary experiments are not shown in this chapter because they are very similar to that of kinetic experiments.

In the computer program, the equilibrium state was defined to have been achieved when the difference between liquid concentration at the external surface of volcanic soil aggregates and that of copper sulfate solution in the bulk liquid is less than 0.000001 ppm. Once this condition is met, the computer stops running the program automatically. At the equilibrium state, the difference calculated by the computer model between liquid concentration at the center of the soil aggregate and that in the bulk liquid will be not greater than 0.0002 ppm.

All results in this chapter, whether from experiments or computer model, were processed and plotted by Excel.

5.2 Thermodynamic studies

The equilibrium adsorption/ desorption plays a dominant role in the fate and transport of heavy metal ions in volcanic soil. It is important to determine the mechanism of the adsorption/desorption equilibrium process. The equilibrium relationship is expressed in terms of isotherms. For heavy metals, the isotherm is dependent on metal and soil properties and environmental conditions.

5.2.1 Adsorption process

The preliminary experiments showed that the equilibrium time for adsorption is eight hours. Thus, all equilibrium experiments for adsorption had been carried out in a shaker for more than eight hours in order to make sure adsorption equilibrium is achieved.

The experiments confirmed that the equilibrium relationship for adsorption could be fitted by the Freundlich isotherm. Figure 5-1 shows the adsorption equilibrium for soil aggregate size of 600-800 μm.

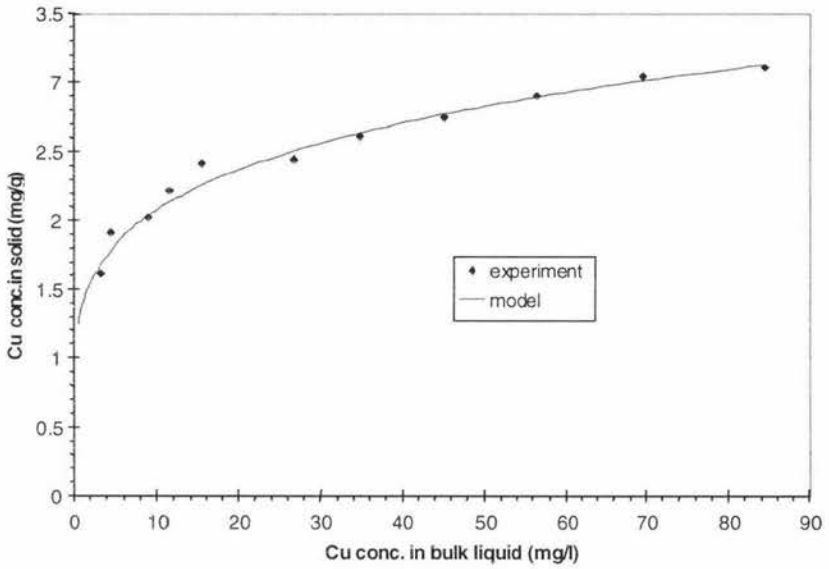

Figure 5-1 Adsorption equilibrium for $CuSO_4$ in volcanic soil of 600-800μm aggregate size

Using the least square method, the following regression equation can be obtained from the experimental data:

$$q = 1.3797C^{\frac{1}{5.4377}} \qquad (600\text{-}800\ \mu m) \qquad (5\text{-}1)$$

The residual value (R^2) for the regression equation is 97.05%. This equation is the equilibrium model that was determined by equilibrium experiments and it has the form of a Freundlich isotherm. The equilibrium constants, K and n, are 1.38 and 5.44,

respectively. The equilibrium parameters (K and n) for adsorption from the experimental data were used in the computer model to predict the equilibrium curve. Running the computer model for different grams of volcanic soil, a set of model data can be given by the computer. Then, the equilibrium curve for the computer model can be plotted by Excel and it is also shown in Figure 5-1. The input parameters of 600-800 μm volcanic soil sample used for the computer model are listed in Table 5-1.

Table 5-1 Inputted kinetic parameters for 600-800 μm aggregate size volcanic soil sample about adsorption equilibrium

items	symbol	values	items	symbol	values
number of nodes	J	21	initial conc. in bulk liquid	Clmin	100.06 ppm
diameter of aggregate	da	0.0007 m	liquid volume	V_l	50 ml
step of time	Δt	1 sec	soil weight	W_t	0.25-5.0g
initial conc. in aggregate	Cmin	0 ppm			

Figure 5-2 and Figure 5-3 show the adsorption experimental results and computer model predictions for volcanic soil aggregate sizes of 500-600 μm and 425-500 μm.

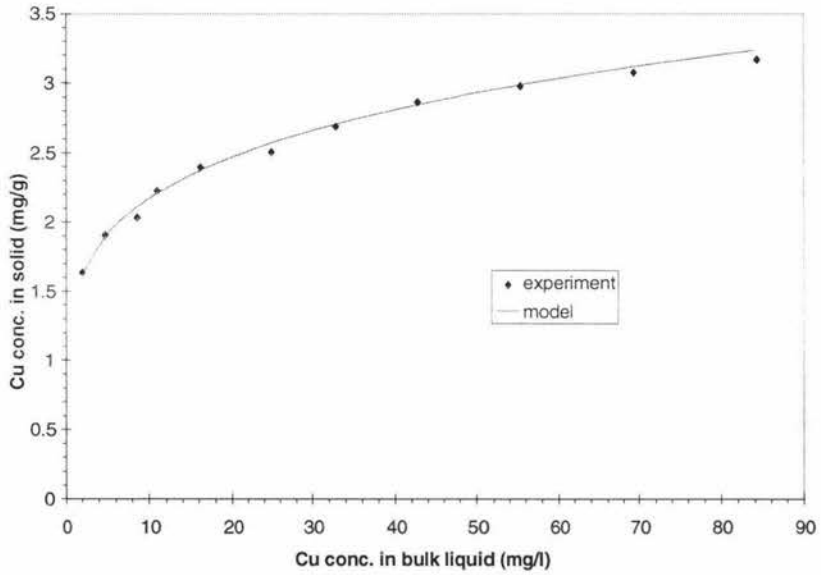

Figure 5-2 Adsorption equilibrium for $CuSO_4$ in volcanic soil of 500-600 μm aggregate size

Equilibrium relationships for these volcanic soil samples are respectively:

$$q = 1.4228C^{\frac{1}{5.4975}} \qquad \text{(500-600 μm)} \qquad (5\text{-}2)$$

$$q = 1.5314C^{\frac{1}{5.8005}} \qquad (425\text{-}500\ \mu m) \qquad (5\text{-}3)$$

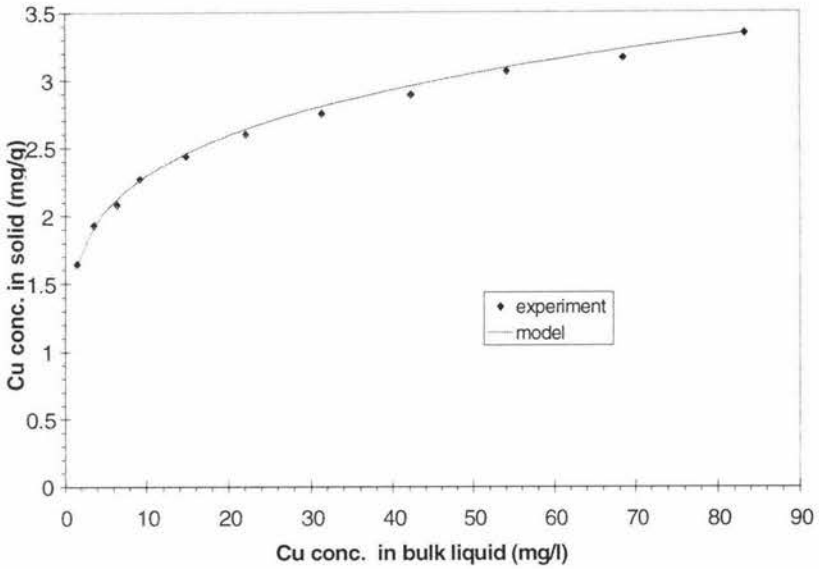

Figure 5-3 Adsorption equilibrium for $CuSO_4$ in volcanic soil of 425-500 μm aggregate size

Table 5-2 shows the adsorption equilibrium constants for different soil aggregate sizes.

Table 5-2 The adsorption equilibrium constants for different soil aggregate sizes

Aggregate size (μm)	K	n
600 ~ 800	1.380	5.438
500 ~ 600	1.423	5.498
425 ~ 500	1.531	5.801

There is a slight difference in equilibrium constants for the Freundlich isotherm for different soil aggregate size. The equilibrium constants for the adsorption process increases with decreasing soil aggregate size. The observed difference in the values of equilibrium constants for the three volcanic soil samples may be due to the experimental errors.

5.2.2 Desorption process

The preliminary experiments showed that the desorption equilibrium time is about

four hours. In order to attain desorption equilibrium, all desorption equilibrium experiments had been carried out in a shaker for more than four hours.

The equilibrium relationships for desorption process are more difficult to obtain than those for adsorption process because they need longer time to be achieved and generally less material is transported. In the equilibrium experiments for the desorption process, an adsorption equilibrium was achieved first, and then the deionized water was used to desorb and a new equilibrium was achieved. The new equilibrium is the desorption equilibrium. Since desorption experiments require prior establishment of adsorption equilibrium, the total length of the desorption experiments is normally much longer than that of adsorption experiments. This could result in damage to the integrity of soil aggregates of volcanic soil, leading to potential errors in desorption data.

The experiments showed that the desorption equilibrium relationship conformed to the Freundlich isotherm. Figure 5-4 shows the desorption equilibrium for soil aggregate size of 600-800 μm.

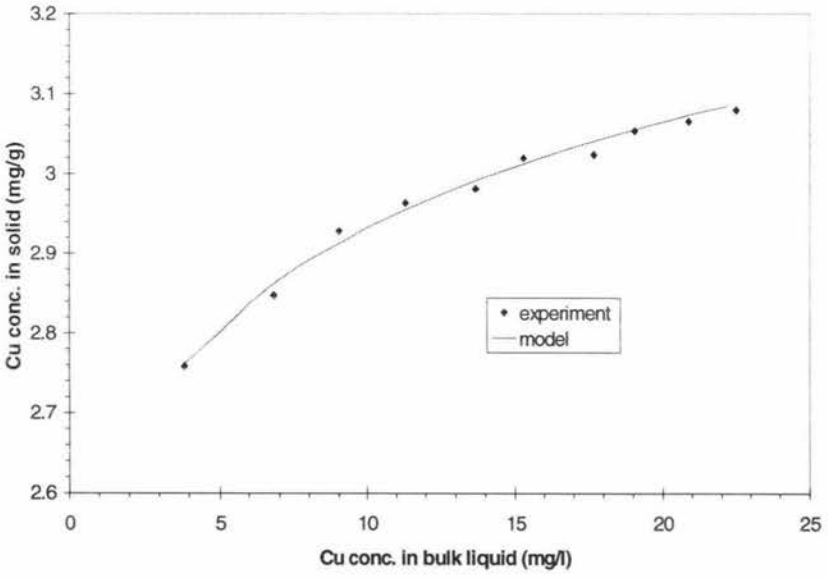

Figure 5-4 Desorption equilibrium for $CuSO_4$ in volcanic soil of 600-800 μm aggregate size

The following regression equation was obtained from the experimental equilibrium

data by using the least square method:

$$q = 2.5379C^{\frac{1}{16.0256}} \qquad (600\text{-}800\ \mu m) \qquad (5\text{-}4)$$

The residual value (R^2) for the regression equation is 99.02%.

The input parameters for 600-800 μm aggregate size volcanic soil used for the computer model are listed in Table 5-3.

Table 5-3 Inputted kinetic parameters for 600-800 μm aggregate size volcanic soil sample about desorption equilibrium

items	symbol	values	items	symbol	values
number of nodes	J	21	initial conc. in bulk liquid	Clmin	0 ppm
diameter of aggregate	da	0.0007 m	liquid volume	V_l	50 ml
step of time	Δt	0.33 sec	soil weight	W_t	0.25-2.5g
initial conc. in aggregate	Cmin	165.21 ppm			

Figure 5-5 and Figure 5-6 show the desorption experimental results and computer model predictions for volcanic soil aggregate sizes of 500-600 μm and 425-500 μm.

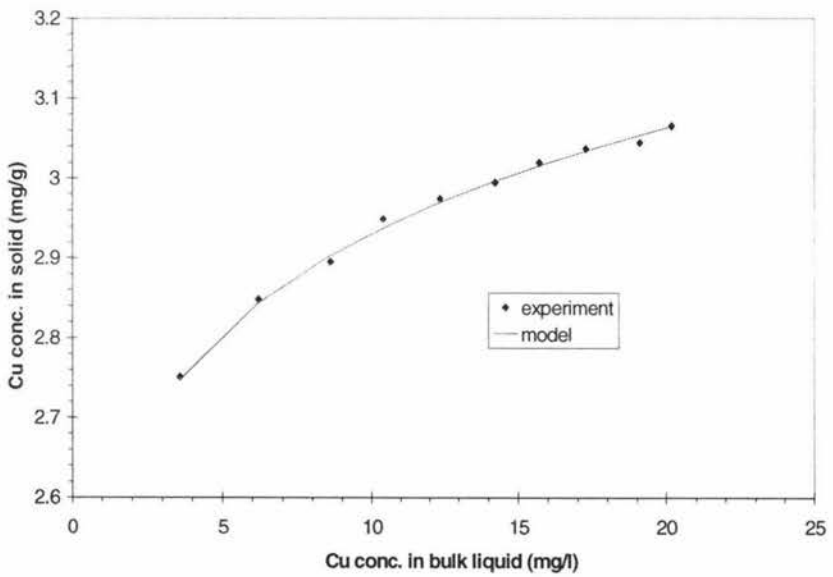

Figure 5-5 Desorption equilibrium for $CuSO_4$ in volcanic soil of 500-600 μm aggregate size

The following two regression equations are for other volcanic soil aggregate sizes of

500-600 μm and 425-500 μm:

$$q = 2.5406C^{\frac{1}{16.0514}} \qquad (500\text{-}600\ \mu m) \qquad (5\text{-}5)$$

$$q = 2.5576C^{\frac{1}{16.6667}} \qquad (425\text{-}500\ \mu m) \qquad (5\text{-}6)$$

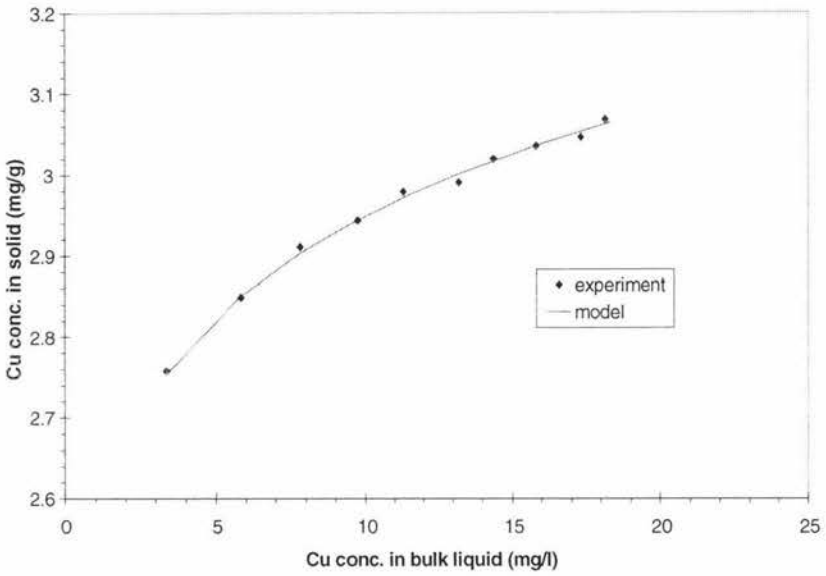

Figure 5-6 Desorption equilibrium for $CuSO_4$ in volcanic soil of 425-500 μm aggregate size

These equilibrium constants for different soil aggregate sizes are listed in Table 5-4.

Table 5-4 The desorption equilibrium constants for different soil aggregate sizes

Aggregate size (μm)	K	n
600 ~ 800	2.538	16.026
500 ~ 600	2.541	16.051
425 ~ 500	2.558	16.667

The Freundlich constant, n, for the desorption process is greater than that for the adsorption process, which means that the desorption equilibrium is different from the adsorption equilibrium. The equilibrium curve for the desorption process is more convex than that for the adsorption process. Therefore, there may be a hysteretic phenomenon between the adsorption process and the desorption process.

Under equilibrium conditions, the concentration of copper sulfate in the bulk liquid for the adsorption process is greater than that for the desorption process with the same amount adsorbed on the solid. Figure 5-7 shows the sketch of adsorption equilibrium curve and desorption equilibrium curve. The heat of adsorption (ΔH) may account for the hysteresis (Adamson, 1990). If the heat of adsorption (ΔH) is not equal to zero, the adsorption activation energy (E_a) will not be equal to the desorption activation energy (E_d), which means that the path of energy change will also be different for different processes, which means that the system is not locally reversible (Adamson, 1990). The copper ions will overcome a different energy barrier from free state to adsorbed state and from adsorbed state to free state. Therefore, the adsorption and desorption path must be different from each other, and the hysteresis must appear. Figure 5-8 shows the relation of the heat of adsorption (ΔH) and activation energy (E_a and E_d). In general, since adsorption is exothermic, the heat of adsorption (ΔH) is greater than zero. Therefore, the desorption activation energy (E_d) must be greater than the adsorption activation energy (E_a), which means that the desorption process of copper ions

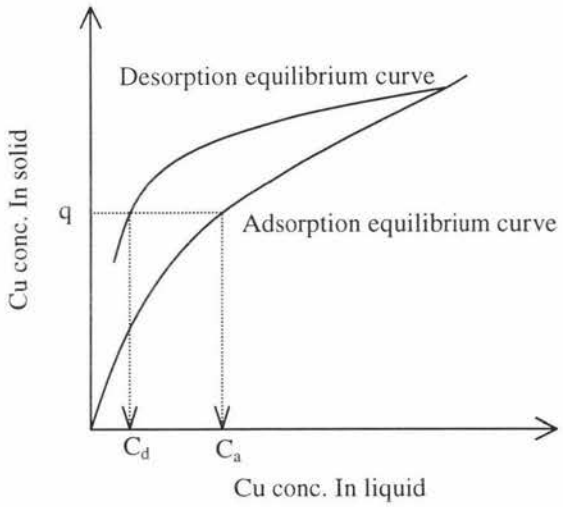

Figure 5-7 Sketch of equilibrium curves of adsorption and desorption

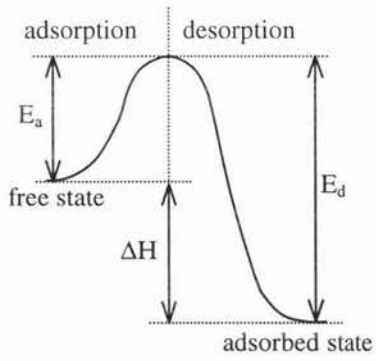

Figure 5-8 Sketch of energy path for adsorption and desorption

adsorbed onto the surface of volcanic soil needs more energy to overcome the potential barrier. Therefore, the desorption process is more difficult to proceed than the adsorption process under the same conditions. Inputting external energy into the system may increase the rate of the desorption process. For example, increasing the temperature of the system by inputting heat energy may accelerate the desorption process.

5.3 Kinetic studies

All studies for kinetic experiments were carried out in flasks as described in Materials and Methods section.

5.3.1 Adsorption process

The kinetic experiments of the adsorption processes were carried out to understand the dynamic for adsorption and desorption.

Figure 5-9 shows the experimental data and model results for 2.5g volcanic soil of 600-800 μm aggregate size contacted with 50 ml of copper sulfate solution:

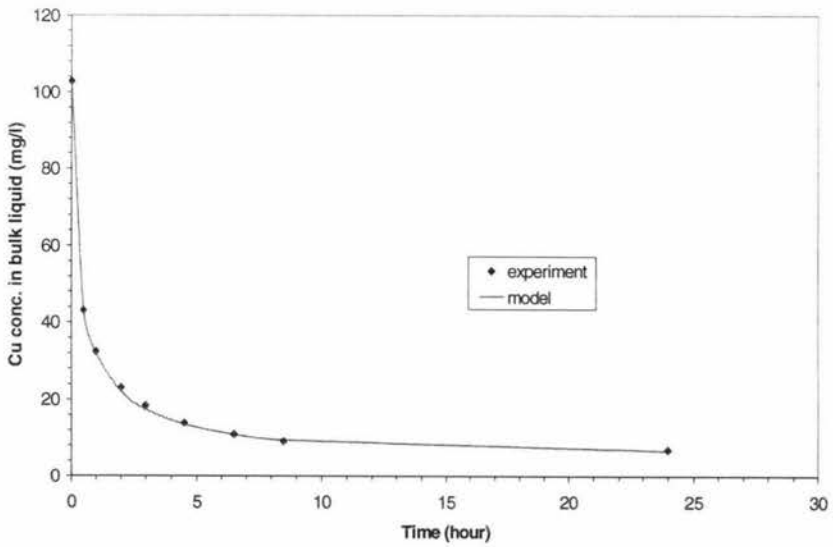

Figure 5-9 Adsorption process for 2.5g volcanic soil of 600-800 μm aggregate size in 50ml $CuSO_4$ solution

The curve for computer model prediction is from inputting the corresponding adsorption equilibrium parameters into the computer program. The input parameters for 600-800 μm aggregate size volcanic soil sample used for the computer model are listed in Table 5-5.

Table 5-5 Inputted kinetic parameters for 600-800 μm aggregate size volcanic soil sample about adsorption kinetic process

items	symbol	values	items	symbol	values
number of nodes	J	21	initial conc. in bulk liquid	Clmin	102.85 ppm
diameter of aggregate	da	0.0007 m	liquid volume	V_l	50 ml
step of time	Δt	1 sec	soil weight	W_t	2.5g
initial conc. in aggregate	Cmin	0 ppm			

Initially, the concentration of copper sulfate in the bulk liquid decreased rapidly. Then, the rate of concentration change gradually slowed down. The transition section continued for about eight to ten hours. Finally, the concentration of copper sulfate in the bulk liquid changed insignificantly, and the adsorption equilibrium was achieved.

Figure 5-10 and Figure 5-11 show the experimental results and computer model predictions for the other two sizes of volcanic soil used:

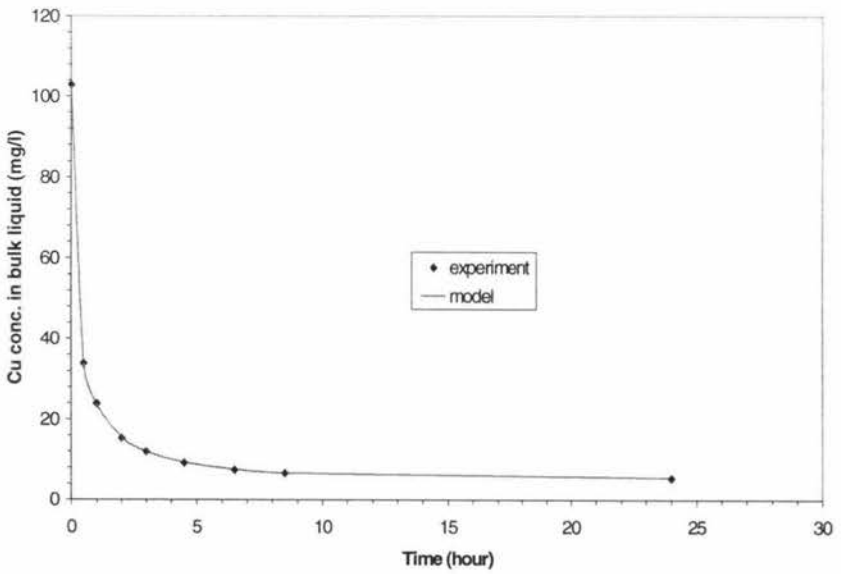

Figure 5-10 Adsorption process for 2.5g volcanic soil of 500-600 μm aggregate size in 50ml CuSO4 solution

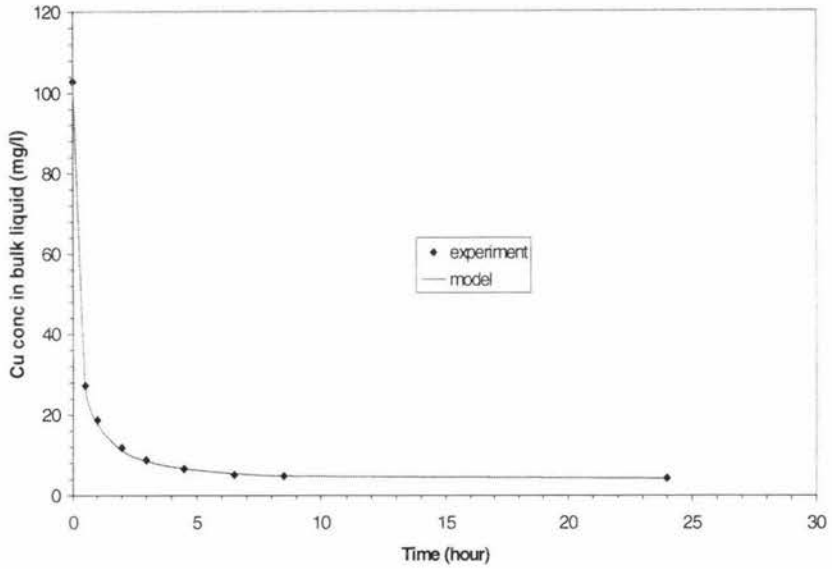

Figure 5-11 Adsorption process for 2.5g volcanic soil of 425-500 μm aggregate size in 50ml $CuSO_4$ solution

The results show that the prediction of the computer model fit the experimental data very well. The curve has a typical two-phase pattern. It has been well documented in literature that adsorption of many heavy metals onto non-volcanic soil or other materials follows a biphasic pattern (Ganguly et al., 1998; Lo and Chen, 1990). The second phase of adsorption was observed to be much longer than the first phase.

The shapes of all three curves are very similar. However, it was found that the smaller the aggregate size of the soil sample, the shorter the transition section of the concentration-decreasing curve was. This suggests that in the system the external mass transfer resistance is negligible. With shorter diffusion path length, the transition time also appears to be shorter.

5.3.2 Desorption process

The kinetic experiments for the desorption process were also carried out twice, However, the soil samples with adsorbed copper sulfate instead of fresh soil samples were used in this experiment. The method of preparing soil samples with adsorbed copper sulfate was expounded in Chapter 3.

Figure 5-12 shows the experimental results and computer model predictions for soil aggregate size of 600-800 μm.

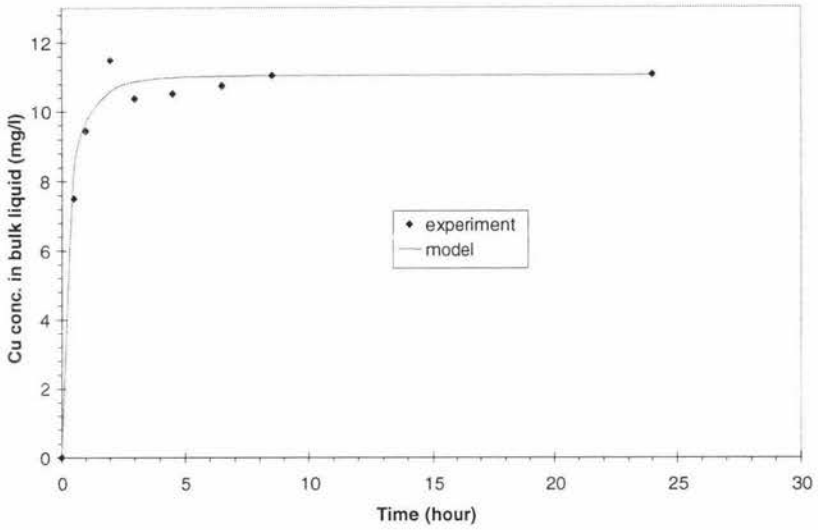

Figure 5-12 Desorption process for 1g volcanic soil of 600-800 μm aggregate size in 50ml deionized water

In order to predict the desorption process, the corresponding equilibrium constants were used. Table 5-6 lists the input parameters for soil aggregate size of 600-800 μm.

Table 5-6 Inputted kinetic parameters for 600-800 μm aggregate size volcanic soil sample about desorption kinetic process

items	symbol	values	items	symbol	values
number of nodes	J	12	initial conc. in bulk liquid	Clmin	0 ppm
diameter of aggregate	da	0.0007 m	liquid volume	V_l	50 ml
step of time	Δt	1 sec	soil weight	W_t	2.5g
initial conc. in aggregate	Cmin	146.8 ppm			

The concentration of copper sulfate in the bulk liquid increases with time, but the transition time of the desorption process is shorter than that for the adsorption process. Because the attraction between copper sulfate becomes weakens gradually, the adsorption rate for copper sulfate at the external layer is slower than that at the first layer or internal layers, which means that the adsorption process will be slower as time progresses before achieving equilibrium at the second phase. This may be the reason why there is a longer transition section on the adsorption curve. In contrast in the desorption process, the copper sulfate at the external layer is released first, and then gradually released from the

upper to the lower layer. Because the external layers of copper sulfate molecules are weakly adsorbed, these tend to desorb more readily. Therefore, the desorption rate is faster and the transition section is shorter than that of the adsorption process.

Figure 5-13 and Figure 5-14 show the experimental results and computer model predictions for soil aggregate size of 500-600 μm and 425-500 μm, respectively.

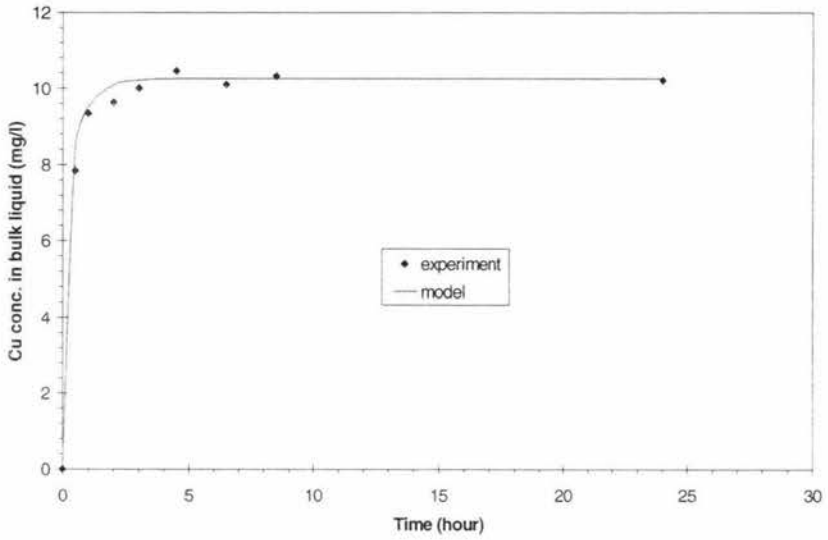

Figure 5-13 Desorption process for 1g volcanic soil of 500-600 μm aggregate size in 50ml deionized water

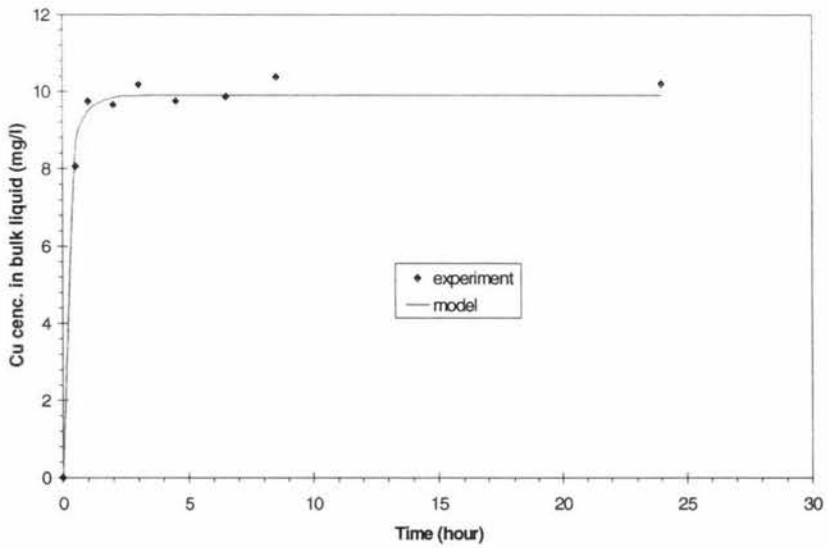

Figure 5-14 Desorption process for 1g volcanic soil of 425-500 μm aggregate size in 50ml deionized water

5.4 Leaching process

Making a computer model to predict the process of leaching heavy metals from volcanic soil in a stirred vessel is the purpose of this project. Experimental data from a stirred vessel experiments was used to verify the computer model. The details of the stirred vessel experiments are given in chapter 3.

Figure 5-15 shows that the experimental results and computer model predictions.

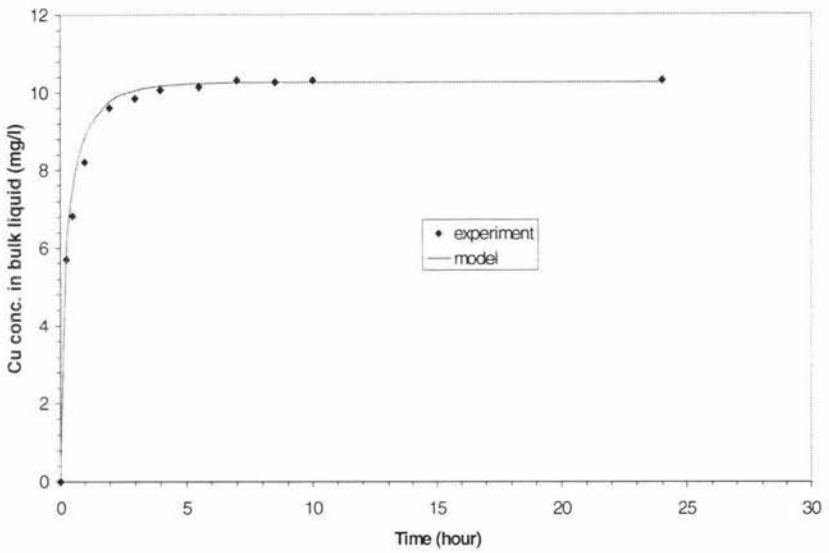

Figure 5-15 Leaching process for 100g volcanic soil of 600-800 μm aggregate size in 5 l deionized water

In this experiment, the equilibrium relationship is the same as that used in the kinetic experiment of the desorption process, but the kinetic parameters are not the same. The input parameters of 600-800 μm aggregate size volcanic soil sample used for the computer model are listed in Table 5-7.

Table 5-7 Inputted kinetic parameters for 600-800 μm aggregate size volcanic soil sample about stirred vessel leaching process

items	symbol	values	items	symbol	values
number of nodes	J	12	initial conc. in bulk liquid	Clmin	0 ppm
diameter of aggregate	da	0.0007 m	liquid volume	V_l	5001.452 ml
step of time	Δt	1 sec	soil weight	W_t	100.0298g
initial conc. in aggregate	Cmin	146.8 ppm			

The experimental results and computer model predictions for soil aggregate size of 500-600 μm and 425-500 μm are shown in Figure 5-16 and Figure 5-17, respectively:

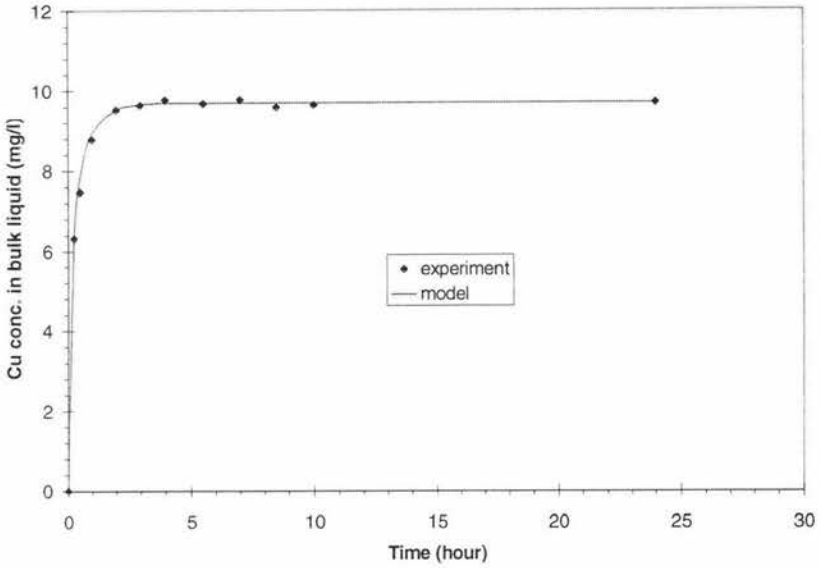

Figure 5-16 Leaching process for 100g volcanic soil of 500-600 μm aggregate size in 5 l deionized water

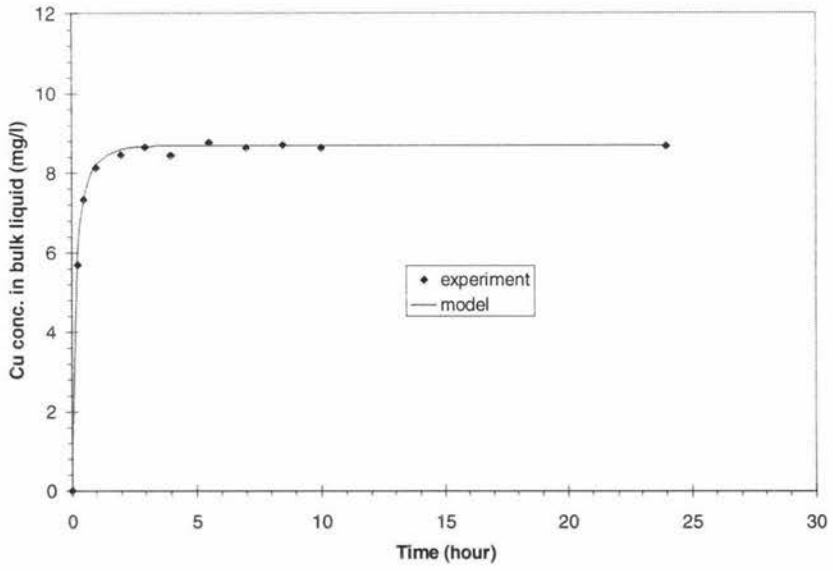

Figure 5-17 Leaching process for 100g volcanic soil of 425-500 μm aggregate size in 5 l deionized water

The experimental results of the stirred vessel experiment agree with the predictions of the computer model well. So the computer model is shown to be reliable.

With the exception of the equilibrium parameters from the experiments, the other computer model parameters were taken from the literature. If the leaching process is for a multi-component mixture of heavy metals instead for a single component, the model needs to be modified incorporating the differential diffusion of the different species.

5.5 Desorption efficiency

Desorption efficiency is a term used to describe the effect of desorption. It is defined by the following equation:

$$\eta = \frac{q_{Mea} - q_{Med}}{q_{Mea}} \tag{5-7}$$

where η the is leaching efficiency (%); q_{Mea} and q_{Med} are the equilibrium amounts of copper sulfate adsorbed onto volcanic soil for adsorption and desorption process respectively and they can be calculated by equation (5-8) and equation (5-9).

$$q_{Mea} = \frac{(C_{M0} - C_{Mea})V_{la}}{W_{sa}} \tag{5-8}$$

where W_{sa} is the mass of volcanic soil used in adsorption process (kg); V_{la} is the volume of liquid for adsorption process (l); C_{M0} is the initial concentration of copper sulfate solution (mg/l); and C_{Mea} is the equilibrium concentration of copper sulfate solution for the adsorption process (mg/l).

$$q_{Med} = q_{Mea} - \frac{C_{Med} \cdot V_{ld}}{W_{sd}} \tag{5-9}$$

where W_{sd} is the mass of volcanic soil used in the desorption process (kg); V_{ld} is the volume of liquid for the desorption process (l); and C_{Med} is the equilibrium concentration of copper sulfate solution for the desorption process (mg/l).

In order to avoid prolonging the time of shaking the mixture of volcanic soil and

solution, the soil sample with adsorbed copper sulfate was prepared by means of fixed bed treatment in this study. Therefore, the mass of volcanic soil and the volume of copper sulfate solution used in the adsorption process are different from those in the desorption process. Desorption efficiency is dependent of the mass of volcanic soil and the volume of deionized water used in the desorption process, which is shown in Figure 5-18.

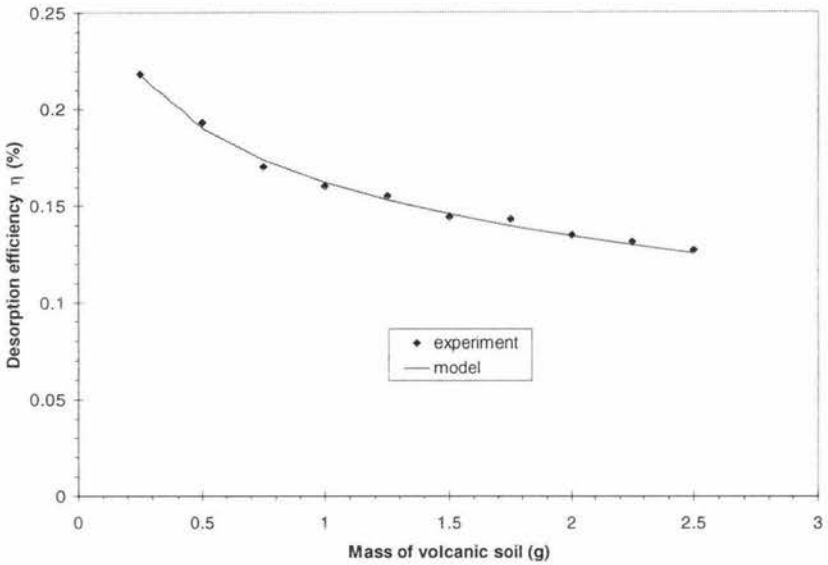

Figure 5-18 Desorption efficiency of different mass of volcanic soil of 600-800 μm size by 50 ml deionized water

Experimental results show that desorption efficiency is quite low at the applied ratio of liquid to solid (20~200 ml/g) used in present study. It was about 12 ~ 22%. Although more water is advantageous to increase the desorption efficiency, too much wastewater from the desorption process needs to be treated and water is a limited resource. Therefore, it may be necessary using acid or organic solvent solutions.

5.6 Control step

Experimental results and computer model predictions show that the process, whether adsorption or desorption of heavy metal in volcanic soil, is controlled by internal diffusion because the rate of the leaching process did not change significantly when the stirring speed changed from 140 rpm to 450 rpm. Figure 5-19 shows the experimental

results and computer model predictions.

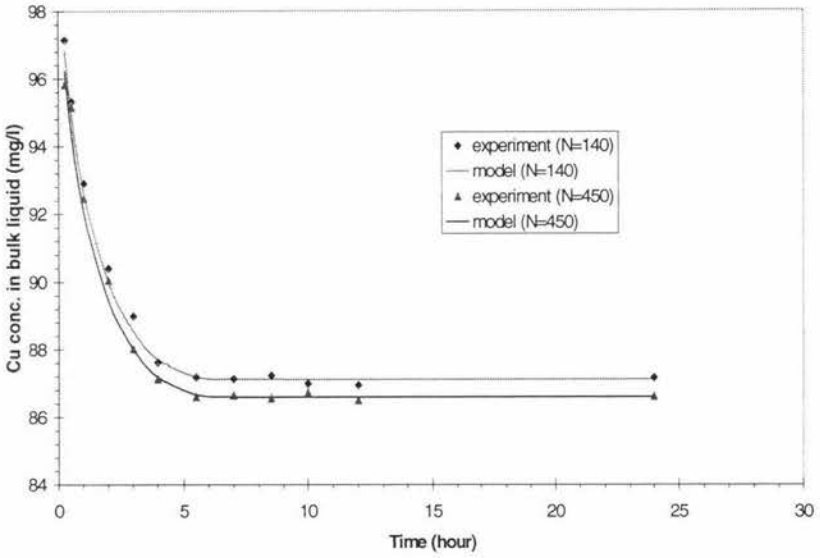

Figure 5-19 Influence of different stirring speeds on the leaching process

The diffusion coefficient of copper sulfate in solution is not constant, but it is a function of the copper concentration. However, its change with concentration is not large, varying from 7.340×10^{-10} to 8.576×10^{-10} m^2/s as the concentration of copper sulfate in bulk liquid changes from 100 ppm to 1 ppm, shown in Table 5-8. Increasing the coefficient of mass transfer in the liquid (k_{lM}) by picking up stirring speed will be of no use to the process because the coefficient of mass transfer (k_{lM}) is much greater than the internal diffusion coefficient in the leaching process. The slower process, internal diffusion, will control the overall rate of leaching. Table 5-8 shows the significant difference between mass transfer coefficient (k_{lM}) and effective internal diffusion coefficient (D_{eM}) of copper sulfate in the aqueous solution with different stirring speeds.

Table 5-8 Comparison of mass transfer coefficient and effective internal diffusion coefficient of CuSO4 in aqueous solution

Stirring speed rpm	**Cu conc.in bulk liquid** ppm	**$k_{lM}\times10^4$** m/s	**$D_{eM}\times10^{10}$** m^2/s
140	1	1.06	8.576
	100	0.96	7.340
450	1	2.09	8.5756
	100	1.89	7.337

In addition, as the stirring speed changed from 140 rpm to 450 rpm, the mass transfer coefficient (k_{lM}) doubled, but the effective internal diffusion coefficient (D_{eM}) only changed marginally. Therefore, the resistance of total mass transfer for the system is mainly concentrated in the interior of the volcanic soil aggregates.

CHAPTER 6

CONCLUSIONS AND RECOMMENDATIONS

6.1 Conclusions

Making a model for predicting the process of leaching heavy metals from volcanic soil is feasible. However, the coefficient of surface diffusion is unknown. In this study, it was neglected, and there is no means of estimating the error due to its neglect. Therefore, increasing the prediction precision of the model may be not significant. Fortunately, ignoring the surface diffusion did not lead to large differences between experiment results and computer model predictions as shown in the preceding chapter. The neglect of surface diffusion is reasonable for this system.

In general, using a batch stirred vessel to leach heavy metals from contaminated soil is a common technology. Therefore, a model, which can simulate the process of leaching heavy metals from volcanic soil successfully, may be used for improving or optimizing the process. Because the difference between experimental data and model data is small, the computer model should be reliable.

The adsorption/desorption equilibrium relationships of copper sulfate on the surface of volcanic soil conformed to the Freundlich isotherm, but the equilibrium constants are different for adsorption and desorption processes. There is a hysteretic phenomenon and the coefficient, n, for desorption is less than that for adsorption. In addition, the rate of attaining equilibrium is greater for desorption and the same metal concentration on the solid particle is maintained by a lower equilibrium bulk concentration in desorption.

The resistance of overall mass transfer for the system is mainly concentrated in the interior of the volcanic soil aggregates. The process, whether adsorption or desorption of

heavy metals in volcanic soil, may be controlled by internal diffusion. Increasing stirring speed will not improve the rate of this process significantly and may damage soil aggregate. Therefore, a fixed bed system may be better than a stirred vessel and save operation cost.

Desorption efficiency is not high just using deionized water to leach copper sulfate from volcanic soil. It was about 12 ~ 22% at a ratio of liquid to solid (20~200 ml/g). Therefore, it may be necessary using an acid or organic solvent solution to replace water as a leaching agent.

No marked change of temperature was observed during the stirring vessel experiment, and the adsorption process is reversible. Therefore, the process is not a chemical adsorption. In addition, it was demonstrated that the adsorption equilibrium conforms to the Freundlich isotherm. The process can be treated as a constant temperature process.

Because the aggregates of volcanic soil are not very strong, in order to decrease the error from soil aggregates breaking up as much as possible, an impeller with bigger external diameter and lower speed should be used.

All kinetic parameters for the model are from the literature, so the model could be used for other heavy metals in a similar situation.

6.2 Recommendations

Improving the prediction precision of the model will result from decreasing the step of space. Because of using the explicit method in this study, the step of time will decrease correspondingly. Thus, the running time of the computer will be longer, especially for the equilibrium data because only one equilibrium data was produced by the computer for each run of the program. In order to plot an equilibrium curve, at least 10 points are needed, which means that the computer program should be run ten times. The implicit method could decrease computer running time and increase the prediction precision.

In the present study, the surface diffusion was neglected because the coefficient of surface diffusion could not be obtained from the literature. However, the neglect is a lack of theoretical basis. In other words, the error from the neglect is on means of estimation. Therefore, it is necessary to develop a formula to calculate the surface diffusion coefficient.

REFERENCES:

Abd-Elfattah, A. and Wada, K. (1981). Adsorption of Lead, Copper, Zinc, Cobalt, and Cadmium by Soils that differ in Cation Exchange Materials. Journal of Soil Science, 32, 271-283.

Adamson, A. W. (1990). Physical Chemistry of Surfaces. (5th ed.). New York: John Wiley and Sons, Inc.

Bielders, C. L., De Backer, L. W. and Delvaux, B. (1990). Particle Density of Volcanic Soils as Measured with A Gas Pycnometer. Soil Science Society of America Journal, 54, 822-826.

Boulding, J. R. (1995). Practical Handbook of Soil, Vadose Zone, and Ground-water Contamination: Assessment, Prevention and Remediation. Boca Raton: Lewis Publishers.

Bromley,L. A. (1973). Thermodynamic Properties of Strong Electrolytes in Aqueous Solutions. American Institute of Chemical Engineers Journal, 19, 313-320.

Brusseau, M. L. and Rao, P. S. C. (1989). Sorption Non-ideality during Organic Contaminant Transport in Porous Media. Crit Review Environmental Control, 19, 33-99.

Childs, C. W., Matsue, N. and Yoshinaga, N. (1991). Ferrihydrite in Volcanic Ash Soils of Japan. Soil Science and Plant Nutrition, 37, 299-311.

Coulson, J. M. and Richardson, J. F. (1979). Chemical Engineering Volume Three. (2nd ed.). Oxford: Pergamon Press.

Cussler, E. L. (1984). Diffusion: Mass Transfer in Liquid Systems. Cambridge: Cambridge University Press.

Egashira, K. and Aomine, S. (1974). Effects of Drying and Heating on the Surface Area of Allophane and Imogolite. Clay Science, 4, 231-242.

Egashira, K., Kaetsu, Y. and Takuma, K. (1983). Aggregate Stability as an Index of Erodibility of Ando soils. Soil Science and Plant Nutrition, 29, 473-482.

FAO/Unesco. (1974). Soil Map of the World, 1:5,000,000. Vol.1, legend. Unesco-Paris.

Ganguly, C., Matsumoto, M. R., Rabideau, J., and Van Benschoten, J. E. (1998). Metal Ion Leaching from Contaminated Soils: Model Calibration and Application. Journal of Emvironmental Engineering. 11, 1150-1158.

Geankoplis, G. J. (1993). Transport Processes and Unit Operation. (3rd ed.). New Jersey: Prentice Hall.

Gibbs, H. S. (1968). Volcanic Ash Soils in New Zealand. In: information series-No. 65, New Zealand Department of Scientific and Industrial Research. Wellington, New Zealand: Soil Bureau, Department of Scientific and Industrial Research.

Gordon, A. R. (1937). The Diffusion Constant of an Electrolyte, and Its Relation to Concentration. Journal of Chemical Physics. 5, 522-526.

Gradwell, M. W. (1974). The Available-water Capacity of Some Southern and Central Zonal Soils of New Zealand. New Zealand Journal of Agricultural Research, 17, 465-478.

Gradwell, M. W. (1976). Available-water Capacity of Some Intrazonal Soils of New Zealand. New Zealand Journal of Agricultural Research, 19, 69-78.

Hall, P. L., Churchman, G. J. and Theng, B. K. G. (1985). Size Distribution of Allophane Unit Particles in Aqueous Suspensions. Clays and Clay Minerals, 33, 345-349.

Harned, H. S. and Owen, B. B. (1950). The Physical Chemistry of Electrolytic Solutions. New York: Reinhold.

Koustas, R. N. and Fischer, D. (1998). Review of separation technologies for treating pesticide-contaminated soil. Journal of The Air and Waste Management Association, 48:5, 434-440.

Leamy, M. L. (1984). Andisols of The World. In: Congresco International de Suelos Volcanicos. Communicaciones. Universida de La Laguna Secretariado de Publicaciones, serie informes 13, (pp. 368-387).

Levenspiel, O. (1972). Chemical Reaction Engineering. (2nd ed.). New York: John Wiley and Sons, Inc.

Levins, D. M. and Glastonbury, J. R. (1972 a). Particle-liquid Hydrodynamics and Mass Transfer in A stirred Vessel, Part I—Particle-liquid Motion. Transactions of The Institutions of Chemical Engineers, 50, 32-41.

Levins, D. M. and Glastonbury, J. R. (1972 b). Particle-liquid Hydrodynamics and Mass Transfer in A stirred Vessel, Part II—Mass Transfer. Transactions of The Institutions of Chemical Engineers, 50, 132-146.

Lo, K. S. L. and Chen, Y. H. (1990). Extracting Heavy Metals from Municipal and Industrial Sludges. The Science of the Total Environment. 90, 99-116.

Lobo, V. M. M. (1984). Electrolyte Solution: Literature Data on Thermodynamic and Transport properties. Portugal: Coimbra.

Lue Hing, C., Zeng, D. R., Sawyer, B., Guth, E. and Whitebloom, S. (1980). Industrial Waste Pretreatment and EPA Cadmium Limitations. Journal Water Pollution Control Federation, 52, 2538-2551.

Mackie, J. S. and Mearres, P. (1955). The Diffusion of Electrolytes in A Cation Exchange Membrane. Proceedings of the Royal Society (London). A232, 498-509.

Maeda, T., Takenaka, H. and Warkentin, B. P. (1977). Physical Properties of Allophane Soils. Advances in Agronomy, 29, 229-264.

McCabe, W. L., Smith, J. C. and Harriott, P. (1993). Unit Operations of Chemical Engineering. (5th ed.). New York: McGraw-Hill.

Nagasawa, K. (1978). Weathering Volcanic Ash and Other Pyroclastic Materials. In: Sudo, T. and Shimoda, S. (eds.), Clays and Clay Materials in Japan, (pp. 105-125). Amsterdam: Elsevier.

Nagasawa, K. and Noro, H. (1987). Mineralogical Properties of Halloysites of Weathering Origin. Chemical Geology, 60, 145-149.

New Zealand Soil Bureau. (1968). Soils of New Zealand: Part 3. In Soil Bureau Bulletin 26(3). Wellington: New Zealand Department of Scientific and Industrial research.

Noll, K. E., Gounaris, V. and Hou, W. (1992). Adsorption Technology for Air and Water Pollution Control. Chelsea, Michigan: Lewis Publishers, Inc.

Ossaka, J. (1982). Activity of Volcanos and Clay Minerals. Nendo Kagaku, 22, 127-137 (in Japanese).

Parfitt, R. L. (1990). Allophane in New Zealand – a review. Australian Journal of Soil Research, 28, 343-360.

Parfitt, R. L. and Childs, C. W. (1983). Comments on Clay Mineralogy of Two Northland Soils New Zealand. Soil Science and Plant Nutrition, 29, 555-559.

Parfitt, R. L. and Webb, T. W. (1984). Allophane in Some South Island Yellow-brown Shallow and Stony Soils and High Country and Upland Yellow-brown Earths. New Zealand Journal of Science, 27, 37-40.

Parfitt, R. L. and Wilson, A. D. (1985). Estimation of Allophane and Halloysite in Three Sequences of Volcanic Soils, New Zealand. In: Caldas, E. F. and Yaalon, D. H. (eds.), Volcanic Soils, 7 (pp. 1-8). Catena Suppl

Parfitt, R. L., Childs, C. W. and Eden, D. N. (1988). Ferrihydrite and Allphoane in Four Andepts from Hawaii and Implications for Their Classification. Geoderma, 41, 223-241.

Perry, R. H. and Green, D. W. (1997). Perry's Chemical Engineers' Handbook. (7th ed.). New York: McGraw-Hill.

Reid, R. C., Prausnitz, J. M. and Poling, B. E. (1987). The Properties of Gases and Liquids. (4th ed.). New York: McGraw-Hill.

Saez, P. B. and Rittmann, B. E. (1992). Model-Parameter Estimation Using Least Squares. Water Research, 26-6, 789-96.

Saigusa, M., Shoji, S. and Kato, T. (1978). Origin and Nature of Halloysite in Ando Soils from Towada Tephra, Japan. Geoderma, 20, 115-129.

Schwertmann, U. and Taylor, R. M. (1989). Iron Oxides. In: Dixon, J. B. and Weed, S. B. (eds.), Minerals in Soils Environments. (2nd ed.), (pp. 379-438). Madison, W1s., USA: Soil Science Society of America.

Shoji, S. (1986). Mineralogical Characteristics. I. Primary minerals. In: Wada, K. (eds.), Ando Soils in Japan, (pp. 21-40). Fukuoka, Japan: Kyushu University Press.

Shoji, S and Ito, T. (1990). Classification of tephra-derived Spodosols. Soil Science, 150, 799-815.

Shoji, S and Masui, J. (1971). Opaline Silica of Resent Volcanic Ash Soils in Japan. Journal of Soil Science, 22, 101-112.

Shoji, S, Nanzyo, M. and Dahlgern, R. (1993). Volcanic Ash Soils: Genesis, Properties and Utilization. Developments in Soil Science 21. Amsterdam: Elsevier.

Slejko, F. L. (1985). Adsorption Technology: A Step-by-Step Approach to Process Evaluation and Application. New York: Marcel Dekker, Inc.

Soil Survey Staff. (1990). Keys to Soil Taxonomy. (4th ed.). AID, USDA-SMSS Technical Monograph No.19, Blacksburg, Virginia.

Soil Survey Staff. (1992). Keys to Soil Taxonomy. (5th ed.). AID, USDA-SMSS Technical Monograph No.19, Blacksburg, Virginia.

Suryaningtyas, D. T. (1998). Characteristics of Volcanic Ash Soils of Southern Area of Mount Ruapehu, North Island, New Zealand. Master thesis in Soil Science, Massey University, Palmerston North, New Zealand.

Susarla, S. (1994) Adsorption-Desorption Characteristics of Phenoxyacetic Acids and Chlorophenols in A Volcanic Soil. Ph.D. thesis, Massey University, Palmerston North, New Zealand.

*Suzuki, and Smith, . (1972). Chemical Engineering Journal. 3, 256-.

Trefry, J. H. and Metz, S. (1984). Selective Leaching of Trace Metals from Sediments as A Function of pH. Analytical Chemistry. 56, 745-749.

Treybal, R. E. (1980). Mass transfer operations. (3rd ed.). New York: McGraw-Hill, Inc.

Van Olphen, H. (1971). Amorphous Clay Materials. Science, 171, 91-92.

Wada, K. (1985). The Distinctive properties of Andisols. Advances in Soil Science, 2, 173-229.

Wada, K. (1989). Allophane and Imogolite. In: Dixon, J. B. and Weed, S. B. (eds.), Minerals in Soils Environments. (2nd ed.). (pp. 1051-1087). Madison, WI: Soil Science Society of America.

Wada, K. and Abd-Elfattah, A. (1978). Characterization of Zinc Adsorption Sites in Two Mineral Soils. Soil Science and Plant Nutrition, 24, 417-426.

Wada, S. –I. and Mizota, C. (1982). Iron-rich Halloysite (10 A) with Crumpled Lamellar Morphology from Hokkaido, Japan. Clays and Clay Minerals, 54, 952-956.

*Wakao, and Smith, . (1962). Chemical Engineering Science. 17, 825-.

Weber, W. J., Jr. (1972). Physicochemical Processes for Water Quality Control. New York: Wiley-Interscuence.

Wu, L., Vomocil, J. A. and Child, S. W. (1990). Pore Size, Particle Size, Aggregate Size, and Water Retention. Soil Science Society of America Journal, 54, 822-826.

Yamamoto, K. (1982). Mechanism of Heavy Metal Sorption by Amorphous Clay Materials. Japanese Soil Science and Plant Nutrition, 53, 355-366.

Yoshinaga, N. and Aomine, S. (1962). Imogolite in Some Ando Soils. Soil Science and Plant Nutrition, 8, 22-29.

Yuan, G. and Lavkulich, L. M. (1997). Sorption Behavior of Copper, Zinc, and Cadmium in Response to Simulated Changes in Soil Properties. Communications in Soil Science and Plant Analysis. 28, 571-587.

APPENDICES:

A1. Liquid film diffusion model

Because there is only one phase in liquid film, no desorption occurs. The mass balance on heavy metal ions for a small element is:

Accumulating rate of H. M. ions at the element	=	The diffusion rate of H. M. ions into the element	-	The diffusion rate of H. M. ions out of the element

Translated the word balance equation to mathematics equation:

$$V\frac{\partial C_M}{\partial t} = A_r \Phi_M - A_{r+dr}(\Phi_M + \frac{\partial \Phi_M}{\partial r}dr) \qquad \text{(A1-1)}$$

A_r and A_{r+dr} are diffusion areas at r and r+dr, respectively. They can be calculated by the following two formulae:

$$A_r = 4\pi \cdot r^2 \qquad \text{(A1-2)}$$

$$A_{r+dr} = 4\pi \cdot (r+dr)^2 \qquad \text{(A1-3)}$$

Substitute equations (A1-2) and (A1-3) into equation (A1-1) and neglect second or higher infinitesimal, equation (A1-1) changes to:

$$V\frac{\partial C_M}{\partial t} = -4\pi \cdot (r^2 \frac{\partial \Phi_M}{\partial r} + 2r \cdot \Phi_M)dr \qquad \text{(A1-4)}$$

V is the volume of the small element and is expressed by following formula:

$$V = \frac{4}{3}\pi \cdot [(r+dr)^3 - r^3] \qquad \text{(A1-5)}$$

Φ_M is the diffusion flux (mg/m^2s), which can be described by Fick's first law:

$$\Phi_M = -D_{IM} \frac{\partial C_M}{\partial r} \tag{A1-6}$$

Substitute equation (A1-5) and equation (A1-6) into equation (A1-4) and divide it by V, and then neglected second or higher infinitesimal, the internal diffusion model can be obtained:

$$\frac{\partial C_M}{\partial t} = \frac{\partial}{\partial r}(D_{IM} \frac{\partial C_M}{\partial r}) + \frac{2D_{IM}}{r} \frac{\partial C_M}{\partial r} \tag{A1-7}$$

where D_M is molecular diffusion coefficient of heavy metal ions in liquid (m^2/s).

Because the liquid film is very thin, a steady concentration distribution of heavy metal ions in liquid film is built quickly. Therefore, equation (A1-7) becomes:

$$0 = \frac{\partial}{\partial r}(D_{IM} \frac{\partial C_M}{\partial r}) + \frac{2D_{IM}}{r} \frac{\partial C_M}{\partial r} \tag{A1-8}$$

Separating variables and integrating, above equation changes to:

$$\ln(D_{IM} \frac{\partial C_M}{\partial r}) = -2 \ln r + c'' \tag{A1-9}$$

The following equation can be obtained by arranging equation (A1-9):

$$c' = r^2 D_{IM} \frac{\partial C_M}{\partial r} \tag{A1-10}$$

where c'' and c' are integral constants. If above equation is timed by 4π, then it becomes:

$$4\pi c' = 4\pi r^2 D_{IM} \frac{\partial C_M}{\partial r} \tag{A1-11}$$

Equation (A1-11) can calculate the amount of mass transfer through a spherical surface

$4\pi r^2$. If it is divided by $4\pi R^2$, Fick's first law based on the exterior surface of a single solid particle can be obtained:

$$\nu_M = -\frac{1}{4\pi R^2}\frac{dn_M}{dt} = -\frac{4\pi r^2}{4\pi R^2} D_{lM} \frac{dC_M}{dr} \qquad \text{(A1-12)}$$

In the liquid film, the range of r is from R to R+δ, so δ is the width of the liquid film. Because R is much greater than δ, ν_M can be regarded as a constant. Therefore, equation (A1-12) can be changed to the following form by separating variables and integrating:

$$\nu_M = \frac{D_{lM}}{\delta}(C_M|_R - C_M|_{R+\delta}) \qquad \text{(A1-13)}$$

Since the width of liquid film is very difficult to be measured, a mass transfer coefficient, k_{lM}, is used often:

$$k_{lM} = \frac{D_{lM}}{\delta} \qquad \text{(A1-14)}$$

Thus, above equation (A1-13) becomes:

$$\nu_M = k_{lM}(C_M|_R - C_M|_{R+\delta}) \qquad \text{(A1-15)}$$

A2. Concentration conversion:

Molality (m) is an alternate concept describing concentration and it is necessary to convert molality into molarity (C). According to the definitions of molality and molarity, they can be expressed by the following equations:

$$C = \frac{n}{V_l} \tag{A2-1}$$

$$m = \frac{n}{W_s} \tag{A2-2}$$

where n is moles of solute; V_l is volume of solution (m^3) and W_s is mass of solvent (kg).

$$\because W_l = V_l \cdot \rho_l = W_s + W_t \tag{A2-3}$$

$$\therefore \frac{C}{\rho_l} = \frac{n}{W_l} = \frac{n}{W_s + W_t} \tag{A2-4}$$

where W_l is mass of solution (kg) and W_t is mass of solute (kg).

$$\because W_t = n \cdot M_t \tag{A2-5}$$

$$\therefore \frac{C}{\rho_l} = \frac{1}{\frac{W_s}{n} + M_t} = \frac{1}{\frac{1}{m} + M_t} \tag{A2-6}$$

where M_t is the molecular weight of solute (kg/kmol). Arrange equation (A2-6) as:

$$m = \frac{1}{\frac{\rho_l}{C} - M_t} \tag{A2-7}$$

A3. Derivation of partial derivative

The molality (m) was used in a formula calculating the diffusion coefficient of an electrolyte (Gordon, 1937). However, only molarity (C) was used in this study, so a derivation of partial derivative was needed. According to the definition of density of solution, it can be expressed as:

$$\rho_l = \frac{W_l}{V_l} = \frac{W_s + W_t}{V_l} = \frac{W_s}{V_l} + \frac{W_t}{V_l} \tag{A3-1}$$

If there is no volume effect as solute dissolves in water or organic solvent, the volume difference between solution and solvent is insignificant.

$$\rho_l \approx \frac{W_s}{V_s} + \frac{W_t}{V_l} = \rho_s + \frac{W_t}{V_l} \tag{A3-2}$$

$$\because \frac{W_t}{V_l} = M_t \cdot C \tag{A3-3}$$

$$\therefore \rho_l \approx \rho_s + M_t \cdot C \tag{A3-4}$$

Substitute equation (A3-4) into equation (A2-7), then the following equation can be derived:

$$m = \frac{C}{\rho_s} \tag{A3-5}$$

$$\therefore I = \frac{C}{\rho_s} \frac{\sum \varphi_i \cdot n_i^{\,2}}{2} \tag{A3-6}$$

Derivation of equation (A3-6):

$$\frac{\partial I}{\partial \ln C} = \frac{\partial I}{\partial C} \cdot \frac{\partial C}{\partial \ln C} = \frac{1}{\rho_s} \frac{\sum \varphi_i \cdot n_i^{\,2}}{2} \cdot C = I \tag{A3-7}$$

$$\because \ln\gamma_{\pm} = |n_+ \cdot n_-| \cdot \ln 10 \cdot [\frac{-0.511\sqrt{I}}{1+\sqrt{I}} + \frac{(0.06+0.6B)\cdot I}{(1+\frac{1.5}{|n_+ \cdot n_-|}I)^2} + \frac{B \cdot I}{|n_+ \cdot n_-|}] \qquad \text{(A3-8)}$$

$$\therefore \frac{\partial \ln\gamma_{\pm}}{\partial \ln m} = |n_+ \cdot n_-| \cdot \ln 10 \cdot [\frac{-0.511\sqrt{I}}{2(1+\sqrt{I})^2} + \frac{(0.06+0.6B)I \cdot (1-\frac{1.5}{|n_+ \cdot n_-|}I)}{(1+\frac{1.5}{|n_+ \cdot n_-|}I)^3} + \frac{B \cdot I}{|n_+ \cdot n_-|}] \qquad \text{(A3-9)}$$

$$\frac{\partial \ln\gamma_{\pm}}{\partial \ln C} = \frac{\partial \ln\gamma_{\pm}}{\partial \ln m} \cdot \frac{\partial \ln m}{\partial \ln C} = \frac{\partial \ln\gamma_{\pm}}{\partial \ln m} \cdot \frac{C}{m}\frac{\partial m}{\partial C} = \frac{\partial \ln\gamma_{\pm}}{\partial \ln m} \cdot \frac{C}{m}\frac{1}{\rho_s} \qquad \text{(A3-10)}$$

Substitute equation (A3-5) into equation (A3-10):

$$\frac{\partial \ln\gamma_{\pm}}{\partial \ln C} = \frac{\partial \ln\gamma_{\pm}}{\partial \ln m} \qquad \text{(A3-11)}$$

A4. Relationship between porosity and densities

According to the definition of porosity, internal porosity (aggregate porosity) can be expressed as:

$$\varepsilon = \frac{V_{at} - V_{ap}}{V_{at}} = \frac{V_{av}}{V_{at}} \tag{A4-1}$$

where V_{at} is the total volume of a single soil aggregate (m^3); V_{ap} is the particle (solid) volume of a single soil aggregate (m^3); V_{av} is the void volume in the soil aggregate (m^3).

If a single volcanic soil aggregate was saturated with solution, the total mass of the single soil aggregate can be expressed as:

$$W_{at} = (V_{at} - V_{av}) \cdot \rho_p + V_{av} \cdot \rho_l \tag{A4-2}$$

$$\because \rho_{as} = \frac{W_{at}}{V_{at}} \tag{A4-3}$$

$$\therefore \rho_{as} = (1-\varepsilon) \cdot \rho_p + \varepsilon \cdot \rho_l \tag{A4-4}$$

where ρ_{as} is the density of soil aggregate saturated by solution or liquid (kg/m^3).

Arrange equation (A4-4), we can get:

$$\varepsilon = \frac{\rho_p - \rho_{as}}{\rho_p - \rho_l} \tag{A4-5}$$

If the soil aggregate is dry, which means that air instead of liquid fills the void of the pore in soil aggregate, the total mass of the single soil aggregate can be expressed as:

$$W_{dat} = (V_{at} - V_{av}) \cdot \rho_p + V_{av} \cdot \rho_g \tag{A4-6}$$

where ρ_g is the density of gas (kg/m^3).

$$\because \rho = \frac{W_{dat}}{V_{at}} \tag{A4-7}$$

$$\therefore \rho = (1-\varepsilon)\cdot\rho_p + \varepsilon\cdot\rho_g \tag{A4-8}$$

where ρ is the density of dry soil aggregate (kg/m^3).

Arrange equation (A4-8), the porosity (ε) can be expressed by the following equation:

$$\varepsilon = \frac{\rho_p - \rho}{\rho_p - \rho_g} \tag{A4-9}$$

Because the density of mineral particles (ρ_p) is much greater than that of air, there is the following relationship:

$$\rho_p - \rho_g \approx \rho_p \tag{A4-10}$$

$$\therefore \varepsilon = \frac{\rho_p - \rho}{\rho_p} \tag{A4-11}$$

A5. Relationship of porosities

The bulk density of volcanic soil is defined as:

$$\varepsilon_b = \frac{V_{ev} + V_{iv}}{V_t} \tag{A5-1}$$

where V_{ev} is the volume of external void (outside of soil aggregate) (m^3); V_{iv} is the volume of internal void (inside of soil aggregate) (m^3); and V_t is the total volume of soil packed (m^3).

The definition of external porosity of packed soil is:

$$\varepsilon_e = \frac{V_{ev}}{V_t} \tag{A5-2}$$

The definition of internal porosity of a single soil aggregate is like Appendix 4.

$$V_t = V_{ev} + n \cdot V_{at} \tag{A5-3}$$

Divide equation (A5-3) by V_t, equation (A5-3) becomes:

$$1 = \varepsilon_e + \frac{nV_{at}}{V_t} \tag{A5-4}$$

$$V_{iv} = n \cdot V_{at}\varepsilon \tag{A5-5}$$

According to the definition of bulk density and substituting equation (A5-5), the following equation can be derived:

$$\varepsilon_b = \frac{V_{ev}}{V_t} + \frac{V_{iv}}{V_t} = \varepsilon_e + \frac{nV_{at}}{V_t}\varepsilon \tag{A5-6}$$

Substitute equation (A5-4) into equation (A5-6), the relationship among the three porosities can be derived:

$$\varepsilon_b = \varepsilon_e + (1-\varepsilon_e)\varepsilon \tag{A5-7}$$